Universität Regensburg
Mathematik

The approximation of planar curve evolutions by stable fully implicit finite element schemes that equidistribute

John W. Barrett, Harald Garcke and Robert Nürnberg

Preprint Nr. 29/2009

The Approximation of Planar Curve Evolutions by Stable Fully Implicit Finite Element Schemes that Equidistribute

John W. Barrett[†] Harald Garcke[‡] Robert Nürnberg[†]

Abstract

Based on earlier work by the authors, in this paper we introduce novel fully discrete, fully practical parametric finite element approximations for geometric evolution equations of curves in the plane. The fully implicit approximations are unconditionally stable and intrinsically equidistribute the vertices at each time level. We present iterative solution methods for the systems of nonlinear equations arising at each time level and present several numerical results. The ideas easily generalize to the evolution of curve networks and to anisotropic surface energies.

Key words. parametric finite elements, equidistributed polygonal meshes, curve evolution, anisotropy, networks of curves, gradient flows

AMS subject classifications. 65M60, 65M12, 35K55, 53C44, 74E10, 74E15

1 Introduction

The parametric finite element approximation of geometric curve evolutions has received great attention over the last two decades. We refer to [1] for a recent overview on geometric evolution equations and their numerical treatment. Beginning with Dziuk's seminal papers [2, 3], almost all of the fully discrete finite element approximations in the literature use a clever semi-implicit discretization that treats most of the geometric quantities explicitly. In general, this then leads to linear systems for the discrete unkowns, which are very similar to the ones arising from standard finite element approximations of one-dimensional partial differential equations on a fixed interval with e.g. periodic boundary conditions. As examples we refer to [3–10], as well as to previous work by the present authors, see [11–13]. The only work on fully implicit finite element approximations that we are aware of is [14], where existence, uniqueness, stability and error bounds are shown for the fully discrete, fully implicit generalization of the semidiscrete scheme in [3] for the curve shortening flow.

[†]Department of Mathematics, Imperial College London, London, SW7 2AZ, UK
[‡]NWF I – Mathematik, Universität Regensburg, 93040 Regensburg, Germany

In the remainder of this introduction we will motivate the fully implicit approximations considered in this paper. As these approximations will lead to equidistributed polygonal discretizations, we also review alternative numerical approaches on equidistributed approximations in the literature. To this end, we introduce the following notation. Let $(\Gamma(t))_{t\in[0,T]}$ be a family of closed curves in the plane, parameterized by $\vec{x} : I \times [0,T] \to \mathbb{R}^2$, $I := \mathbb{R}/\mathbb{Z}$. With s denoting arclength of $\Gamma(t)$, we can define the unit tangent $\vec{x}_s(\rho,t) = \frac{\vec{x}_\rho(\rho,t)}{|\vec{x}_\rho(\rho,t)|}$, $\rho \in I$, and the unit normal $\vec{\nu} = -\vec{x}_s^{\perp}$, where $\cdot^{\perp}$ denotes a clockwise rotation through 90°. All of the considerations in this section remain valid for the alternative normal $\vec{x}_s^{\perp}$. However, with a view towards introducing general anisotropies later on in this paper, we will fix the stated sign convention throughout.

In order to keep the presentation simple, in this introduction we will restrict ourselves to the two geometric evolution equations of (a) curve shortening flow, also called curvature flow, and (b) surface diffusion

$$\text{(a)} \quad \mathcal{V} = \varkappa \qquad \text{and} \qquad \text{(b)} \quad \mathcal{V} = -\varkappa_{ss}\,, \tag{1.1}$$

where $\mathcal{V} := \vec{x}_t \,.\, \vec{\nu}$ is the normal velocity of $\Gamma(t)$, and $\varkappa$ denotes its curvature, i.e.

$$\varkappa\,\vec{\nu} = \vec{\varkappa} := \vec{x}_{ss}\,. \tag{1.2}$$

Clearly, (1.1a) is a highly nonlinear partial differential equation of second order, while (1.1b) describes a fourth order flow. It is not difficult to show that solutions to (1.1a,b) satisfy

$$\text{(a)} \quad \frac{\mathrm{d}}{\mathrm{d}t}\,|\Gamma(t)| = -\int_{\Gamma(t)} \varkappa^2 \,\mathrm{d}s \qquad \text{and} \qquad \text{(b)} \quad \frac{\mathrm{d}}{\mathrm{d}t}\,|\Gamma(t)| = -\int_{\Gamma(t)} (\varkappa_s)^2 \,\mathrm{d}s\,, \tag{1.3}$$

where

$$|\Gamma(t)| := \int_{\Gamma(t)} 1 \,\mathrm{d}s = \int_I |\vec{x}_\rho| \,\mathrm{d}\rho \tag{1.4}$$

defines the length of the curve. In particular, we see that the curve shortening flow (1.1a) is the L^2-gradient flow of (1.4), while the surface diffusion flow (1.1b) is the H^{-1}-gradient flow of (1.4), and as such it conserves the area enclosed by Γ.

Most of the numerical approaches for the approximation of (1.1a,b) in the literature do not control the tangential distribution of mesh points, and so to prevent numerical singularities such as coalescense or swallow tails, i.e. numerically induced self-intersections, in practice mesh smoothing methods in general need to be employed. See e.g. [7, 8, 15] for possible mesh smoothing strategies. The application of such remeshing methods is usually viewed as undesirable. For example, they might smoothen the solution excessively, stability results that hold for the original approximation are in general lost, and when applied to approximations of (1.1b) great care must be taken to ensure that the mesh smoothing method conserves the enclosed area. Hence for a long time there has been interest in deriving numerical discretization methods that intrinsically maintain a good mesh quality. Here one possible approach is to consider numerical methods, where the nodes of the polygonal approximations of $\Gamma(t)$ remain equidistributed throughout.

The first such approach that we are aware of was introduced in [16], see also [17], for the second order flow (1.1a) and generalizations of it to the movement of phase boundaries in solidification problems. Here the basic idea is to only consider parameterizations that satisfy

$$|\vec{x}_\rho(\rho,t)| = |\Gamma(t)| \qquad \forall\ \rho \in I\,,\ t \in [0,T]\,, \tag{1.5a}$$

which means that ρ (up to a constant) is arclength, and then to reformulate (1.1a) in terms of an evolution equation for the tangential angle ϑ, where

$$\vec{x}_s = (\cos\vartheta, \sin\vartheta)\,, \tag{1.5b}$$

and so $\varkappa = \vartheta_s$. The solution $\vartheta(\rho,t)$ can then be used to integrate (1.5b) in order to obtain the curve parameterization $\vec{x}(\rho,t)$, and this idea has since been used by a number of authors, see e.g. [18, 19], and also [20] for a slightly different variant. We remark that when (1.5b) is integrated on the discrete level, then the resulting approximation of $\vec{x}(\rho,t)$ will in general not be equidistributed. In [18] the author uses a special integration rule to ensure equidistribution for a periodic interface, but as this violates the periodicity on the discrete level, his approach does not appear to generalize to closed curves. A second possible approach, which appears to have been first considered in [21, 22] for the flow (1.1a), is to discretize an evolution equation for the position vector $\vec{x}$ in the form

$$\vec{x}_t = \mathcal{V}\,\vec{\nu} + \alpha\,\vec{x}_s\,, \tag{1.6a}$$

where the tangential velocity α is chosen such that the nodes of the triangulation remain close to being equidistributed. However, rather then choosing a continuous velocity α, the author in [21, 22] adds a heuristic tangential velocity on the discrete level, which is effective in trying to locate the points uniformly, and hence prevent coalescence. The authors in [23,24], on the other hand, consider the formulation (1.6a) for the flows (1.1a,b) and a fixed choice for α. In particular, they show that choosing α such that

$$\alpha_s = \mathcal{V}\,\varkappa - \frac{1}{|\Gamma(t)|}\int_{\Gamma(t)} \mathcal{V}\,\varkappa\,\mathrm{d}s \tag{1.6b}$$

implies that $\left(\frac{|\vec{x}_\rho(\rho,t)|}{|\Gamma(t)|}\right)_t = 0$, and so ρ (up to a constant) is arclength if $\vec{x}(\rho,0)$ is an arclength parameterization of $\Gamma(0)$. The authors then discretize (1.6a,b) with the help of finite differences, leading to linear systems of equations to be solved at each time level. We note that the fully discrete approximations of the formulation (1.6a) will in general not be equidistributed. In addition, we mention that the variational approach in [4] for the curve shortening flow (1.1a), see also [5], can be viewed as approximating (1.6a) with $\alpha = |\vec{x}_\rho|^{-3}\,(\vec{x}_{\rho\rho}\,.\,\vec{x}_\rho)$. Although this choice of tangential velocity in general does not lead to an arclength parameterization of $\Gamma(t)$, in practice these authors observed well distributed polygonal approximations.

Finally, the authors in [25], see also [26], supplement the flow equations (1.1a,b) with the side constraint

$$\vec{x}_\rho(\rho,t)\,.\,\vec{x}_{\rho\rho}(\rho,t) = 0 \qquad \forall\ \rho \in I\,,\ t \in (0,T]\,, \tag{1.7}$$

which, on noting that $(\frac{1}{2}\,|\vec{x}_\rho|^2)_\rho = \vec{x}_\rho \,.\, \vec{x}_{\rho\rho}$, is equivalent to (1.5a). The authors then introduce a finite difference approximation to (1.1a,b) with (1.7), which leads to a system of nonlinear equations at each time level. On approximating (1.7) fully implicitly with the help of centred finite differences, the authors obtain an equidistribution property on the discrete level, although this is not explicitly stated in their work. In addition, their numerical method is extended to the case of evolving curve networks, see [25] for details.

Before we introduce the novel approach considered in this paper, we sumarize that what all of the above approaches (1.5a,b), (1.6a,b) and (1.7) have in common is that a suitable reformulation of (1.1a,b) is considered, which enforces $\vec{x}(\rho,t)$ to be an arclength parameterization of $\Gamma(t)$. Whether this property is reflected on the discrete level, however, i.e. whether the vertices of the polygonal approximations to $\Gamma(t)$ are uniformly spaced, depends subtly on the chosen time and space discretizations. Apart from the approach in [25], the fully discrete approximations of the numerical approaches discussed so far, applied to evolving closed curves, will in general not be equidistributed. Naturally, in practice this is of little importance and presented numerical results are in general close to being equidistributed, see [16–26] for more details. In addition we note that so far there does not seem to be a stability analysis available for any of the fully discrete approximations of the previously discussed numerical approaches, e.g. in the spirit of (1.3).

The approach considered in this paper makes use of the following weak formulation of (1.1a,b) with (1.2), that was first introduced by the authors in [11] in order to derive parametric finite element approximations of (1.1b) for curves and curve networks in the plane. Given $\Gamma(0) = \vec{x}(I,0)$, for all $t \in (0,T]$ find $\Gamma(t) = \vec{x}(I,t)$, with $\vec{x}(t) \in H^1(I,\mathbb{R}^2)$, and $\varkappa(t) \in H^1(I,\mathbb{R})$ such that

$$\begin{aligned} &\text{(a)} \quad \int_{\Gamma(t)} (\vec{x}_t \,.\, \vec{\nu})\,\varphi \,\mathrm{d}s - \begin{cases} \int_{\Gamma(t)} \varkappa\,\varphi \,\mathrm{d}s \\ \int_{\Gamma(t)} \varkappa_s\,\varphi_s \,\mathrm{d}s \end{cases} = 0 \qquad \forall\ \varphi \in H^1(I,\mathbb{R})\,, \qquad (1.8)\\ &\text{(b)} \quad \int_{\Gamma(t)} \varkappa\,\vec{\nu} \,.\, \vec{\varphi} \,\mathrm{d}s + \int_{\Gamma(t)} \vec{x}_s \,.\, \vec{\varphi}_s \,\mathrm{d}s = 0 \qquad \forall\ \vec{\varphi} \in H^1(I,\mathbb{R}^2)\,. \qquad (1.9) \end{aligned}$$

It is the variational formulation (1.9) of the identity (1.2) that will be at the core of the equidistribution property exhibited by the fully discrete approximations introduced in this paper. Of course, the idea of using a variational formulation of (1.2) in order to design a numerical method for the approximation of (1.1a,b) is not new. In fact, the idea goes back to Dziuk's seminal paper [2], and has since been used by a number of authors in order to derive finite element approximations of (1.1a,b) and more general flows; see e.g. [3, 5, 7, 8, 10].

Several remarks on (1.9) are due. First of all, we note that intriguingly, and in contrast to the previously discussed approaches (1.5a,b), (1.6a,b) and (1.7), the formulation (1.8a,b) with (1.9) does not enforce any condition on the tangential velocity $\alpha = \vec{x}_t \,.\, \vec{x}_s$ of $\vec{x}$ and, in particular, ρ need not be an arclength parameterization. In fact, it is easy to see that the tangential velocity of $\vec{x}$ is indeed arbitrary, and so there does not exist a unique solution to (1.8a,b) with (1.9). However, on replacing $H^1(I,\mathbb{R})$ and $H^1(I,\mathbb{R}^2)$ with conforming piecewise linear finite element spaces, one can derive a semidiscrete continuous-in-time approximation of (1.8a,b), (1.9) that will equidistribute the vertices

of the approximations to $\Gamma(t)$, where these approximations are not locally flat, and from now on we will refer to this property as weak equidistribution. See the Remark 2.4 in [11], where the novel variational formulation (1.9) was introduced by the present authors for the first time. Based on the idea of this semidiscrete approximation, in the series of papers [11–13], the present authors have introduced fully discrete parametric finite element approximations to (1.1a,b) that are unconditionally stable and that have good mesh properties in practice. These fully discrete schemes use a semi-implicit time stepping discretization, which, as discussed previously, is standard in the literature, and which leads to simple linear systems of equations at each time level. However, the semi-implicit time stepping means that although in practice the observed mesh quality is very good, the (weak) equidistribution property that holds for the semidiscrete scheme will in general not hold for the fully discrete, semi-implicit approximations.

Building on this earlier work, it is the aim of this paper to introduce fully discrete, fully implicit finite element approximations of (1.8a,b), (1.9) that are unconditionally stable and that satisfy the (weak) equidistribution property of the semidiscrete scheme at each time step. Apart from being much simpler than the previously discussed numerical methods, we believe that these are the first unconditionally stable fully discrete approximations of the geometric evolution equations (1.1a,b) in the literature, for which an equidistribution property can be shown. Moreover, the presented ideas immediately carry over to the case of evolving curve networks and to anisotropic surface energies. Naturally, these novel approximations will no longer lead to linear systems. To the contrary, as the schemes are now fully implicit, the resulting algebraic equations are highly nonlinear. Hence appropriate nonlinear solution methods need to be developed, in order to compute solutions to the introduced finite element approximations.

We conclude this introduction with two further remarks on the variational formulation (1.9) of the identity (1.2). On assuming that $\vec{x}(\rho,t)$ is an arclength parameterization of $\Gamma(t)$, the equation (1.9) can be equivalently formulated as

$$\int_I \varkappa\, \vec{x}_\rho^{\,\perp} \,.\, \vec{\varphi}\,\mathrm{d}\rho - \frac{1}{|\Gamma(t)|}\int_I \vec{x}_\rho \,.\, \vec{\varphi}_\rho\,\mathrm{d}\rho = 0 \qquad \forall\ \vec{\varphi} \in H^1(I,\mathbb{R}^2)\,. \tag{1.10}$$

Conversely, it is easy to see that (1.10) implies (1.7), and hence any solution to (1.8a,b), (1.10) also solves (1.8a,b), (1.9), and in particular is an arclength solution. It will turn out that one of the fully discrete approximations introduced in this paper can be viewed as a discrete analogue of (1.8a,b) with (1.10); see Remark 2.3 below. For these and some related schemes, the weak equidistribution property discussed above can be replaced with strong equidistribution at each time level, i.e. the vertices of the approximations to $\Gamma(t)$ will be uniformly spaced no matter whether the approximations are locally flat or not. However, when deriving fully discrete finite element approximations it is advisable and indeed beneficial to always consider the original variational formulation (1.8a,b), (1.9), rather than (1.8a,b), (1.10). Then also semi-implicit approximations are unconditionally stable and curve shortening, and generalizations to anisotropic surface energies, to the evolution of curve networks in the plane and to the evolution of hypersurfaces and surface clusters in $\mathbb{R}^3$ are easily possible. In this context we recall that (1.9) is naturally extended to hypersurfaces in $\mathbb{R}^3$. In the series of papers [27–30] this has been employed

by the authors to introduce fully practical, semi-implicit finite element approximations for geometric evolution equations of surfaces and surface clusters in $\mathbb{R}^3$, which in general maintain a very good mesh quality. Here it is worth noting that none of the approaches (1.5a,b), (1.6a,b) or (1.7) generalizes to the treatment of surfaces in $\mathbb{R}^3$.

The remainder of this paper is organized as follows. In Section 2 we introduce fully discrete, fully implicit finite element approximations of (1.8a,b), (1.9) and prove stability and equidistribution properties. These schemes are generalized to the treatment of curve networks and to anisotropic surface energies in §2.1 and §2.2, respectively. In Section 3 we present iterative solution methods for the highly nonlinear systems of equations that arise at each time step of the fully implicit finite element approximations. Finally, in Section 4 we present numerical experiments for the novel finite element approximations introduced in this paper. These results clearly exhibit the equidistribution property established in Section 2, and we present comparisons with results from semi-implicit finite element schemes introduced by the authors in earlier work.

2 Finite Element Approximation

We introduce the decomposition $I = \cup_{j=1}^{J} I_j$, $J \geq 3$, of $I = \mathbb{R}/\mathbb{Z}$ into intervals given by the nodes q_j, $I_j = [q_{j-1}, q_j]$. For later use, we assume that the subintervals form an equipartitioning of I, i.e. that

$$q_j = j\,h\,, \quad \text{with} \quad h := J^{-1}\,, \qquad j = 0 \to J\,. \tag{2.1}$$

Throughout this paper, we make use of the periodicity of I, i.e. $q_J \equiv q_0$, $q_{J+1} \equiv q_1$ and so on. The necessary finite element spaces are now defined as follows

$$\underline{V}_0^h := \{\vec{\chi} \in C(I, \mathbb{R}^2) : \vec{\chi}|_{I_j} \text{ is linear } \forall\ j = 1 \to J\} =: [V_0^h]^2 \subset H^1(I, \mathbb{R}^2),$$

where $V_0^h \subset H^1(I, \mathbb{R})$ is the space of scalar continuous (periodic) piecewise linear functions, with $\{\chi_j\}_{j=1}^{J}$ denoting the standard basis of V_0^h. Let $0 = t_0 < t_1 < \ldots < t_{M-1} < t_M = T$ be a partitioning of $[0, T]$ into possibly variable time steps $\tau_m := t_{m+1} - t_m$, $m = 0 \to M-1$. We set $\tau := \max_{m=0\to M-1} \tau_m$. Given $\Gamma^0 = \vec{X}^0(I)$, our fully discrete approximations will define a sequence of polygonal curves Γ^m, $m = 0 \to M$, where $\Gamma^m = \vec{X}^m(I)$ with $\vec{X}^m \in \underline{V}_0^h$. For scalar and vector valued functions $u, v \in L^2(I, Z)$, with $Z = \mathbb{R}$ or $Z = \mathbb{R}^2$, we define the L^2-inner product $\langle u, v\rangle_I := \int_I u\,.\,v\,\mathrm{d}\rho$, and, for the case that u, v are piecewise continuous, we also define the mass lumped inner product $\langle u, v\rangle_I^h := \frac{h}{2}\sum_{j=1}^{J}\left[(u\,.\,v)(q_j^-) + (u\,.\,v)(q_{j-1}^+)\right]$, where $u(q_j^{\pm}) := \lim_{\varepsilon \searrow 0} u(q_j \pm \varepsilon)$, and where we have recalled (2.1). In addition, we define the shorthand notations $\langle u, v\rangle_{\Gamma^m} := \langle u\,.\,v, |\vec{X}_\rho^m|\rangle_I$ and $\langle u, v\rangle_{\Gamma^m}^h := \langle u\,.\,v, |\vec{X}_\rho^m|\rangle_I^h$.

Let $\vec{\nu}^m := -(\vec{X}_s^m)^\perp = -|\vec{X}_\rho^m|^{-1}\,(\vec{X}_\rho^m)^\perp$. Moreover, let $\vec{\omega}^m \in \underline{V}_0^h$ be defined by setting

$$\vec{\omega}^m(q_j) := \begin{cases} \vec{0} & \vec{X}^m(q_{j-1}) = \vec{X}^m(q_j) = \vec{X}^m(q_{j+1}) \\ \frac{-[\vec{X}^m(q_{j+1}) - \vec{X}^m(q_{j-1})]^\perp}{|\vec{X}^m(q_j) - \vec{X}^m(q_{j-1})| + |\vec{X}^m(q_{j+1}) - \vec{X}^m(q_j)|} & \text{otherwise} \end{cases},$$

for $j = 1 \to J$. Then it is easy to see that

$$\langle \vec{v}, w\,\vec{\omega}^m\rangle^h_{\Gamma^m} = \langle \vec{v}, w\,\vec{\nu}^m\rangle^h_{\Gamma^m} = -\langle \vec{v}, w\,(\vec{X}^m_\rho)^\perp\rangle^h_I \qquad \forall\ \vec{v} \in \underline{V}^h_0,\ w \in V^h_0\,. \tag{2.2}$$

For later use, we also define the polygonal edges

$$\vec{h}^m_j := \vec{X}^m(q_{j+1}) - \vec{X}^m(q_j)\,, \quad j = 1 \to J\,. \tag{2.3}$$

We propose the following approximation to (1.1a,b): For $m \geq 0$, given $\vec{X}^m \in \underline{V}^h_0$, find $\Gamma^{m+1} = \vec{X}^{m+1}(I)$, with $\vec{X}^{m+1} \in \underline{V}^h_0$, and $\kappa^{m+1} \in V^h_0$ such that

$$\begin{matrix}\text{(a)}\\ \text{(b)}\end{matrix} \qquad \langle \frac{\vec{X}^{m+1} - \vec{X}^m}{\tau_m}, \chi\,\vec{\omega}^{m+1}\rangle^h_{\Gamma^{m+1}} - \begin{cases}\langle \kappa^{m+1}, \chi\rangle^h_{\Gamma^{m+1}}\\ \langle \kappa^{m+1}_s, \chi_s\rangle_{\Gamma^{m+1}}\end{cases} = 0 \qquad \forall\ \chi \in V^h_0\,, \tag{2.4}$$

$$\langle \kappa^{m+1}\,\vec{\omega}^{m+1}, \vec{\eta}\rangle^h_{\Gamma^{m+1}} + \langle \vec{X}^{m+1}_s, \vec{\eta}_s\rangle_{\Gamma^{m+1}} = 0 \qquad \forall\ \vec{\eta} \in \underline{V}^h_0\,. \tag{2.5}$$

Of course, on eliminating κ^{m+1}, the system (2.4a), (2.5) can be equivalently written as

$$\langle \frac{\vec{X}^{m+1} - \vec{X}^m}{\tau_m}\,.\,\vec{\omega}^{m+1}, \vec{\eta}\,.\,\vec{\omega}^{m+1}\rangle^h_{\Gamma^{m+1}} + \langle \vec{X}^{m+1}_s, \vec{\eta}_s\rangle_{\Gamma^{m+1}} = 0 \qquad \forall\ \vec{\eta} \in \underline{V}^h_0\,. \tag{2.6}$$

REMARK. 2.1. *We remark that the schemes* (2.4a), (2.5) *and* (2.4b), (2.5) *are fully implicit versions of the following two semi-implicit approximations to the flows* (1.1a,b), *which the authors introduced in [12] and [11], respectively. For* $m \geq 0$, *given* $\Gamma^m = \vec{X}^m(I)$, *with* $\vec{X}^m \in \underline{V}^h_0$, *find* $\Gamma^{m+1} = \vec{X}^{m+1}(I)$, *with* $\vec{X}^{m+1} \in \underline{V}^h_0$, *and* $\kappa^{m+1} \in V^h_0$ *such that*

$$\begin{matrix}\text{(a)}\\ \text{(b)}\end{matrix} \qquad \langle \frac{\vec{X}^{m+1} - \vec{X}^m}{\tau_m}, \chi\,\vec{\omega}^m\rangle^h_{\Gamma^m} - \begin{cases}\langle \kappa^{m+1}, \chi\rangle^h_{\Gamma^m}\\ \langle \kappa^{m+1}_s, \chi_s\rangle_{\Gamma^m}\end{cases} = 0 \qquad \forall\ \chi \in V^h_0\,, \tag{2.7}$$

$$\langle \kappa^{m+1}\,\vec{\omega}^m, \vec{\eta}\rangle^h_{\Gamma^m} + \langle \vec{X}^{m+1}_s, \vec{\eta}_s\rangle_{\Gamma^m} = 0 \qquad \forall\ \vec{\eta} \in \underline{V}^h_0\,. \tag{2.8}$$

We note that (2.7a), (2.8) *and* (2.7b), (2.8) *are linear and recall from [11, 12] that existence, uniqueness and stability for these approximations can be shown under some mild assumptions on the old polygonal curves* Γ^m.

REMARK. 2.2. *The fully implicit scheme from [14], which is based on the semidiscrete approximation of* (1.1a) *introduced in [3], reads: For* $m \geq 0$, *given* $\vec{X}^m \in \underline{V}^h_0$, *find* $\Gamma^{m+1} = \vec{X}^{m+1}(I)$, *with* $\vec{X}^{m+1} \in \underline{V}^h_0$, *such that*

$$\langle \frac{\vec{X}^{m+1} - \vec{X}^m}{\tau_m}, \vec{\eta}\rangle^h_{\Gamma^{m+1}} + \langle \vec{X}^{m+1}_s, \vec{\eta}_s\rangle_{\Gamma^{m+1}} = 0 \qquad \forall\ \vec{\eta} \in \underline{V}^h_0\,. \tag{2.9}$$

In [14] existence, uniqueness, stability and error bounds are shown for (2.9), *and so the analysis of* (2.9) *is much more developed than what at present appears possible for* (2.6). *A key difference between* (2.9) *and* (2.6) *is that the former will in general not equidistribute the vertices of* Γ^{m+1}, *and in practice coalescence of vertices can be observed for nontrivial evolutions.*

The following theorem states stability estimates for the fully implicit, fully discrete schemes (2.4a,b), (2.5).

THEOREM. 2.1. *Let* $(\vec{X}^m, \kappa^m)_{m=1}^M$ *be a solution of* (2.4a), (2.5). *Then for all* $k = 1 \to M$ *we have that*

$$\begin{matrix}\text{(a)}\\ \text{(b)}\end{matrix} \qquad |\Gamma^k| + \sum_{m=0}^{k-1} \tau_m \begin{cases} \langle \kappa^{m+1}, \kappa^{m+1} \rangle_{\Gamma^{m+1}}^h \\ \langle \kappa_s^{m+1}, \kappa_s^{m+1} \rangle_{\Gamma^{m+1}} \end{cases} \leq |\Gamma^0| \,. \tag{2.10}$$

Proof. Choosing $\chi = \kappa^{m+1} \in V_0^h$ in (2.4a) and $\vec{\eta} = \frac{\vec{X}^{m+1} - \vec{X}^m}{\tau_m} \in \underline{V}_0^h$ in (2.5) yields that

$$\langle \vec{X}_s^{m+1}, \vec{X}_s^{m+1} - \vec{X}_s^m \rangle_{\Gamma^{m+1}} + \tau_m \, \langle \kappa^{m+1}, \kappa^{m+1} \rangle_{\Gamma^{m+1}}^h = 0 \,. \tag{2.11}$$

We now analyse the first term in (2.11). On recalling (2.3), it holds that

$$\begin{aligned} \langle \vec{X}_s^{m+1}, \vec{X}_s^{m+1} - \vec{X}_s^m \rangle_{\Gamma^{m+1}} &= \int_{\Gamma^{m+1}} \vec{X}_s^{m+1} \,.\, (\vec{X}_s^{m+1} - \vec{X}_s^m) \, \mathrm{d}s \\ &= \sum_{j=1}^J \left[\frac{|\vec{h}_j^{m+1}|^2 - \vec{h}_j^{m+1} \,.\, \vec{h}_j^m}{|\vec{h}_j^{m+1}|} \right] \geq \sum_{j=1}^J \left[|\vec{h}_j^{m+1}| - |\vec{h}_j^m| \right] = |\Gamma^{m+1}| - |\Gamma^m| \,. \end{aligned} \tag{2.12}$$

Combining (2.11) and (2.12) yields that

$$|\Gamma^{m+1}| - |\Gamma^m| + \tau_m \, \langle \kappa^{m+1}, \kappa^{m+1} \rangle_{\Gamma^{m+1}}^h \leq 0 \,. \tag{2.13}$$

Summing (2.13) for $m = 0 \to k-1$ yields the desired result (2.10a). The proof of (2.10b) is analogous. ∎

We remark for the interested reader that while the approximations (2.4a,b), (2.5) immediately carry over to the case of evolving hypersurfaces in $\mathbb{R}^3$, see [27] for the relevant details, it does not seem possible to then generalize the stability results in Theorem 2.1 to this higher dimensional case.

THEOREM. 2.2. *Let* $(\vec{X}^{m+1}, \kappa^{m+1})$ *denote a solution to* (2.4a,b), (2.5). *Then it holds that*

$$|\vec{h}_j^{m+1}| = |\vec{h}_{j-1}^{m+1}| \quad \textit{if} \quad \vec{h}_j^{m+1} \not\parallel \vec{h}_{j-1}^{m+1} \,, \qquad j = 1 \to J \,. \tag{2.14}$$

Proof. The proof is analogous to the proof in [11, Remark 2.4] for the semidiscrete variant of (2.4b), (2.5). Fix an arbitrary $j \in \{1, \ldots, J\}$. If $\vec{h}_j^{m+1} = \vec{0}$, $\vec{h}_{j-1}^{m+1} = \vec{0}$ or $\vec{h}_j^{m+1} + \vec{h}_{j-1}^{m+1} = \vec{0}$, then the claim (2.14) trivially holds. In all the other cases we obtain, on choosing $\vec{\eta} = [\vec{\omega}^{m+1}(q_j)]^\perp \, \chi_j$ in (2.5) and on noting that $[\vec{\omega}^{m+1}(q_j)]^\perp = \frac{\vec{h}_j^{m+1} + \vec{h}_{j-1}^{m+1}}{|\vec{h}_j^{m+1}| + |\vec{h}_{j-1}^{m+1}|}$, that

$$0 = \left(\frac{\vec{h}_j^{m+1}}{|\vec{h}_j^{m+1}|} - \frac{\vec{h}_{j-1}^{m+1}}{|\vec{h}_{j-1}^{m+1}|} \right) . \left(\vec{h}_j^{m+1} + \vec{h}_{j-1}^{m+1} \right) = \frac{|\vec{h}_j^{m+1}| - |\vec{h}_{j-1}^{m+1}|}{|\vec{h}_j^{m+1}| \, |\vec{h}_{j-1}^{m+1}|} \left(|\vec{h}_j^{m+1}| \, |\vec{h}_{j-1}^{m+1}| - \vec{h}_j^{m+1} \,.\, \vec{h}_{j-1}^{m+1} \right) . \tag{2.15}$$

Clearly, (2.15) and the Cauchy-Schwarz inequality imply that $|\vec{h}_j^{m+1}| = |\vec{h}_{j-1}^{m+1}|$ if $\vec{h}_j^{m+1}$ is not parallel to $\vec{h}_{j-1}^{m+1}$. ∎

In view of Theorem 2.2, we also consider the following adaptations of our schemes (2.4a,b), (2.5). For $m \geq 0$, given $\vec{X}^m \in \underline{V}_0^h$, find $\Gamma^{m+1} = \vec{X}^{m+1}(I)$, with $\vec{X}^{m+1} \in \underline{V}_0^h$, and $\kappa^{m+1} \in V_0^h$ such that

$$\begin{aligned} &\text{(a)} \quad \langle \frac{\vec{X}^{m+1} - \vec{X}^m}{\tau_m}, \chi\,(\vec{X}_\rho^{m+1})^\perp \rangle_I^h + \begin{cases} |\Gamma^{m+1}|\,\langle \kappa^{m+1}, \chi \rangle_I^h \\ |\Gamma^{m+1}|^{-1}\,\langle \kappa_\rho^{m+1}\,\chi_\rho \rangle_I \end{cases} = 0 \qquad \forall\ \chi \in V_0^h\,, \quad (2.16) \\ &\text{(b)} \quad \langle \kappa^{m+1}\,(\vec{X}_\rho^{m+1})^\perp, \vec{\eta} \rangle_I^h - |\Gamma^{m+1}|^{-1}\,\langle \vec{X}_\rho^{m+1}, \vec{\eta}_\rho \rangle_I = 0 \qquad \forall\ \vec{\eta} \in \underline{V}_0^h\,. \quad (2.17) \end{aligned}$$

These reformulations will prove particularly useful when introducing iterative solution methods for the nonlinear systems (2.4a,b), (2.5). See Section 3 for details.

THEOREM. 2.3. *Let $(\vec{X}^m, \kappa^m)_{m=1}^M$ denote a solution to* (2.16a,b), (2.17). *Then it holds that*

$$|\vec{h}_j^{m+1}| = |\vec{h}_{j-1}^{m+1}|\,, \qquad j = 1 \to J\,, \quad m = 0 \to M-1\,. \tag{2.18}$$

In addition, $(\vec{X}^m, \kappa^m)_{m=1}^M$ is a solution to (2.4a,b), (2.5). *In particular, the stability results* (2.10a,b) *hold. Conversely, if $(\vec{X}^{m+1}, \kappa^{m+1})$ is a solution to* (2.4a,b), (2.5) *such that Γ^{m+1} is truly equidistributed, then it also solves* (2.16a,b), (2.17).

Proof. Fix an arbitrary $j \in \{1, \ldots, J\}$. If $\vec{\omega}^{m+1}(q_j) = \vec{0}$, then the claim (2.18) trivially holds. In all the other cases we obtain, on choosing $\vec{\eta} = [\vec{\omega}^{m+1}(q_j)]^\perp\,\chi_j$ in (2.17) and on recalling (2.2), that

$$0 = \left(\vec{h}_j^{m+1} - \vec{h}_{j-1}^{m+1}\right) . \left(\vec{h}_j^{m+1} + \vec{h}_{j-1}^{m+1}\right) = |\vec{h}_j^{m+1}|^2 - |\vec{h}_{j-1}^{m+1}|^2\,. \tag{2.19}$$

This proves (2.18). The remaining claims then follow on noting (2.2) and that (2.18) and (2.1) imply that $|\Gamma^{m+1}|\,\langle \chi, \eta \rangle_I^h = \langle \chi, \eta\,|\vec{X}_\rho^{m+1}| \rangle_I^h = \langle \chi, \eta \rangle_{\Gamma^{m+1}}^h$ and $|\Gamma^{m+1}|^{-1}\,\langle \chi_\rho, \eta_\rho \rangle_I = \langle \chi_\rho, \eta_\rho\,|\vec{X}_\rho^{m+1}|^{-1} \rangle_I = \langle \chi_s, \eta_s \rangle_{\Gamma^{m+1}}$ for all $\chi, \eta \in V_0^h$; and similarly for vector valued functions $\vec{\chi}$, $\vec{\eta} \in \underline{V}_0^h$. □

REMARK. 2.3. *We observe that apart from providing a definition of the discrete curvature κ^{m+1}, the equation* (2.17) *can be interpreted as a weak formulation of the side constraint*

$$\vec{X}_\rho^{m+1} \,.\, \vec{X}_{\rho\rho}^{m+1} = 0\,; \tag{2.20}$$

recall also (1.10). *In this respect, the schemes* (2.16a,b), (2.17) *are not dissimilar to the approach suggested in [25] for the evolution of closed curves and curve networks. In fact, using centred finite differences in* (2.20) *immediately yields* (2.19), *although this is not stated in [25].*

REMARK. 2.4. *Existence of solutions to any of the schemes* (2.4a,b), (2.5) *and* (2.16a,b), (2.17) *is an open problem. It does not appear possible to use a fixed point argument with the help of e.g. the Brouwer fixed point theorem. Here the hope would be to show existence of a solution on assuming that $|\Gamma^m| > 0$ and that τ_m is sufficiently small. However, as there is no immediate control of the tangential component of $\vec{X}^{m+1} - \vec{X}^m$ available, it does not appear to be possible to exclude a priori the possibility that ∂_s degenerates on Γ^{m+1} for the*

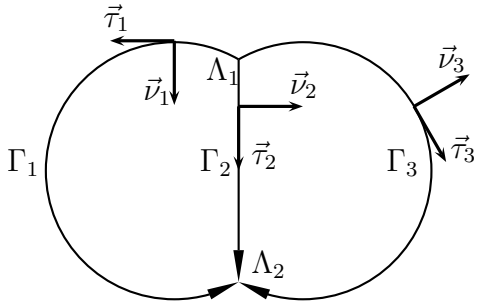

Figure 1: The setup of $\Gamma = (\Gamma_1, \Gamma_2, \Gamma_3)$.

schemes (2.4a,b), (2.5), *as would happen when* $\vec{h}_j^{m+1} = \vec{0}$ *for a* $j \in \{1, \dots, J\}$. *Of course, the reformulations* (2.16a,b), (2.17) *do not suffer from the same problem. However, once again it does not appear possible to apply e.g. the Brouwer fixed point theorem, as there does not appear to be a priori knowledge which would prevent the degenerate case* $|\Gamma^{m+1}| = 0$. *Hence it is difficult to establish coercivity of the discrete nonlinear operator. Naturally, in practice these considerations are not very relevant. Indeed, our iterative solvers always managed to find a solution in situations that are away from singularities of the continuous flow, such as extinctions for the curve shortening flow.*

So far in this paper we have limited our attention to the curve evolutions (1.1a,b) for a closed curve in the plane. We chose these simple setups in order to highlight the novelty of the fully implicit approximations and their properties. However, it is now straightforward to combine these new presented ideas to other curve evolutions that were previously studied by the authors. Below we will outline the details for some of these cases. In particular, the ideas carry across to the approximation of curve shortening flow and surface diffusion of curve networks, [11, 12], to anisotropic evolution equations, [31], to curve evolutions in higher codimensions and geodesic flows on manifolds, [13], as well as to the approximation of phase boundary movements in solidification processes, [32].

2.1 Curve networks

For simplicity, here we consider the simple setup as in Figure 1; cf. [12, Fig. 1]. That is, we want to numerically approximate gradient flows for

$$|\Gamma(t)| = \sum_{i=1}^{3} |\Gamma_i(t)| \,, \tag{2.21}$$

where $\Gamma = (\Gamma_1, \Gamma_2, \Gamma_3)$ is the simplified curve network under consideration. We remark that for the L^2- and H^{-1}-gradient flows of (2.21) we obtain

$$\text{(a)} \quad \mathcal{V}_i = \varkappa_i \,, \quad i = 1 \to 3 \,, \qquad \text{and} \qquad \text{(b)} \quad \mathcal{V}_i = -(\varkappa_i)_{ss} \,, \quad i = 1 \to 3 \,, \tag{2.22}$$

respectively, together with conditions that need to hold at the two triple junction points Λ_1 and Λ_2. Here $\mathcal{V}_i$ is the normal velocity of $\Gamma_i(t)$, and $\varkappa_i$ denotes its curvature. Mixed flows of the form

$$\mathcal{V}_1 = \varkappa_1 \,, \qquad \mathcal{V}_i = -(\varkappa_i)_{ss} \,, \quad i = 2 \to 3 \,, \tag{2.23}$$

which have applications in the modelling of the sintering of powder components, [33], thermal grooving, [34], interface motions in polycrystalline two-phase materials, [35], and in the modelling of the evolution of boundaries in the electromigration of intergranular voids, [36], can also be considered. We refer to [12] for details on these flows and on the necessary triple junction conditions.

Let $[0,1] = \bigcup_{j=1}^{J_i} I_j^i$, $i = 1 \to 3$, be decompositions of $[0,1]$ into intervals $I_j^i = [q_{j-1}^i, q_j^i]$ based on the nodes $\{q_j^i\}_{j=0}^{J_i}$, $J_i \geq 2$. Similarly to (2.1), we assume that $q_j^i = j/J_i$, $j = 0 \to J_i$, $i = 1 \to 3$. Let $\underline{V} := \{(\vec{\chi}_1, \vec{\chi}_2, \vec{\chi}_3) \in [C([0,1], \mathbb{R}^2)]^3 : \vec{\chi}_1 = \vec{\chi}_2 = \vec{\chi}_3 \text{ on } \{0,1\}\}$, $V := \{(\chi_1, \chi_2, \chi_3) \in [C([0,1], \mathbb{R})]^3\}$ and $W := \{(\chi_1, \chi_2, \chi_3) \in [C([0,1], \mathbb{R})]^3 : \chi_1 + \chi_2 + \chi_3 = 0 \text{ on } \{0,1\}\}$. The appropriate finite element spaces are then defined by $\underline{V}^h := \{\vec{\chi} \in \underline{V} : \vec{\chi}_i \mid_{I_j^i} \text{ is linear } \forall\ j = 1 \to J_i,\ i = 1 \to 3\}$, and similarly for the spaces of scalar functions $V^h \subset V$ and $W^h \subset W$. Moreover, we introduce the L^2-inner product $\langle \cdot, \cdot \rangle_{\Gamma^m}$ and the mass lumped inner product $\langle \cdot, \cdot \rangle_{\Gamma^m}^h$ over the curve network $\Gamma^m := (\Gamma_1^m, \Gamma_2^m, \Gamma_3^m)$, which is described by the vector function $\vec{X}^m \in \underline{V}^h$, for scalar and vector valued functions $u, v \in [L^2([0,1], Z)]^3$, with $Z = \mathbb{R}$ or $Z = \mathbb{R}^2$, as follows: $\langle u, v \rangle_{\Gamma^m} := \sum_{i=1}^3 \langle u_i, v_i \rangle_{\Gamma_i^m} := \sum_{i=1}^3 \langle u_i \,.\, v_i, |[\vec{X}_i^m]_\rho| \rangle_{[0,1]}$ and $\langle u, v \rangle_{\Gamma^m}^h := \sum_{i=1}^3 \langle u_i, v_i \rangle_{\Gamma_i^m}^h := \sum_{i=1}^3 \langle u_i \,.\, v_i, |[\vec{X}_i^m]_\rho| \rangle_{[0,1]}^h$. We then propose the following approximations for the two gradient flows (2.22a,b). For $m \geq 0$, given $\vec{X}^m \in \underline{V}^h$, find $\Gamma^{m+1} = \vec{X}^{m+1}([0,1])$, with $\vec{X}^{m+1} \in \underline{V}^h$, and (a) $\kappa^{m+1} \in V^h$, or (b) $\kappa^{m+1} \in W^h$, such that

$$\begin{matrix} \text{(a)} \\ \text{(b)} \end{matrix} \qquad \langle \frac{\vec{X}^{m+1} - \vec{X}^m}{\tau_m}, \chi\, \vec{\nu}^{m+1} \rangle_{\Gamma^{m+1}}^h - \begin{cases} \langle \kappa^{m+1}, \chi \rangle_{\Gamma^{m+1}}^h \\ \langle \kappa_s^{m+1}, \chi_s \rangle_{\Gamma^{m+1}} \end{cases} = 0 \qquad \forall\ \chi \in \begin{cases} V^h \\ W^h \end{cases}, \tag{2.24}$$

$$\langle \kappa^{m+1}\, \vec{\nu}^{m+1}, \vec{\eta} \rangle_{\Gamma^{m+1}}^h + \langle \vec{X}_s^{m+1}, \vec{\eta}_s \rangle_{\Gamma^{m+1}} = 0 \qquad \forall\ \vec{\eta} \in \underline{V}^h\,. \tag{2.25}$$

We note that (2.24a,b), (2.25) are the obvious fully implicit analogues of the semi-implicit approximations introduced in [11, 12]. Moreover, extending these approximations to the mixed flow (2.23) is straightforward, see [12] for details. It is then not difficult to generalize the results in Theorem 2.1 and Theorem 2.2 to the above approximations for curve networks. To this end, we introduce the polygonal edges $\vec{h}_j^{m,i} := \vec{X}_i^m(q_{j+1}^i) - \vec{X}_i^m(q_j^i)$, $j = 1 \to J_i$, $i = 1 \to 3$.

THEOREM. 2.4. *Let $(\vec{X}^m, \kappa^m)_{m=1}^M$ be a solution of* (2.24a,b), (2.25). *Then for all $k = 1 \to M$ we have that*

$$\begin{matrix} \text{(a)} \\ \text{(b)} \end{matrix} \qquad |\Gamma^k| + \sum_{m=0}^{k-1} \tau_m \begin{cases} \langle \kappa^{m+1}, \kappa^{m+1} \rangle_{\Gamma^{m+1}}^h \\ \langle \kappa_s^{m+1}, \kappa_s^{m+1} \rangle_{\Gamma^{m+1}} \end{cases} \leq |\Gamma^0|\,. \tag{2.26}$$

Proof. The proof is analogous to the proof of Theorem 2.1. ∎

THEOREM. 2.5. *Let $(\vec{X}^{m+1}, \kappa^{m+1})$ denote a solution to* (2.24a,b), (2.25). *Then it holds that*

$$|\vec{h}_j^{m+1,i}| = |\vec{h}_{j-1}^{m+1,i}| \quad \text{if} \quad \vec{h}_j^{m+1,i} \not\parallel \vec{h}_{j-1}^{m+1,i}\,, \qquad j = 1 \to J_i\,,\ i = 1 \to 3\,. \tag{2.27}$$

Proof. The proof is analogous to the proof of Theorem 2.2. ☐

Similarly to (2.16a,b), (2.17), we can now derive truly equidistributing variants of (2.24a,b), (2.25) as follows. For $m \geq 0$, given $\vec{X}^m \in \underline{V}^h$, find $\Gamma^{m+1} = \vec{X}^{m+1}([0,1])$, with $\vec{X}^{m+1} \in \underline{V}^h$, and (a) $\kappa^{m+1} \in V^h$, or (b) $\kappa^{m+1} \in W^h$, such that

$$\begin{aligned} &\text{(a)} \quad \langle \frac{\vec{X}^{m+1} - \vec{X}^m}{\tau_m}, \chi\, \vec{\nu}^{m+1} \rangle^h_{\Gamma^{m+1}} - \sum_{i=1}^{3} \begin{cases} |\Gamma_i^{m+1}|\, \langle \kappa^{m+1}, \chi \rangle^h_{[0,1]} \\ |\Gamma_i^{m+1}|^{-1} \langle (\kappa_i^{m+1})_\rho, (\chi_i)_\rho \rangle_{[0,1]} \end{cases} = 0 \quad \forall\, \chi \in \begin{cases} V^h \\ W^h, \end{cases} \\ &\text{(b)} \end{aligned} \tag{2.28}$$

$$\langle \kappa^{m+1}\, \vec{\nu}^{m+1}, \vec{\eta} \rangle^h_{\Gamma^{m+1}} + \sum_{i=1}^{3} |\Gamma_i^{m+1}|^{-1}\, \langle (\vec{X}_i^{m+1})_\rho, (\vec{\eta}_i)_\rho \rangle_{[0,1]} = 0 \qquad \forall\, \vec{\eta} \in \underline{V}^h\,. \tag{2.29}$$

Once again we observe that (2.29) can be interpreted as including a weak formulation of the side constraints $(\vec{X}_i^{m+1})_\rho \,.\, (\vec{X}_i^{m+1})_{\rho\rho} = 0$, $i = 1 \to 3$. These constraints appear in the system of partial differential algebraic equations considered in [25]. But we stress that an advantage of (2.28a,b), (2.29), and its generalization to the mixed flow (2.23), is that the triple junction conditions are naturally taken care of, while the finite difference framework considered in [25] necessitates the use of ghost points.

THEOREM. 2.6. *Let $(\vec{X}^m, \kappa^m)_{m=1}^M$ denote a solution to* (2.28a,b), (2.29). *Then it holds that*

$$|\vec{h}_j^{m+1,i}| = |\vec{h}_{j-1}^{m+1,i}|\,, \qquad j = 1 \to J_i\,,\ i = 1 \to 3\,, \quad m = 0 \to M-1\,. \tag{2.30}$$

In addition, $(\vec{X}^m, \kappa^m)_{m=1}^M$ is a solution to (2.24a,b), (2.25) *and, in particular, the stability result* (2.26a,b) *holds. Conversely, if $(\vec{X}^{m+1}, \kappa^{m+1})$ is a solution to* (2.24a,b), (2.25) *such that Γ_i^{m+1} is truly equidistributed for $i = 1 \to 3$, then it also solves* (2.28a,b), (2.29).

Proof. The proof is analogous to the proof of Theorem 2.3. ☐

2.2 Anisotropic surface energies

Based on the authors' work in [31], we will now introduce fully implicit finite element approximations of gradient flows for closed planar curves for an anisotropic surface energy. An anisotropic surface energy has the form

$$|\Gamma(t)|_\gamma := \int_{\Gamma(t)} \gamma(\vec{\nu})\ \mathrm{d}s\,, \tag{2.31}$$

where $\gamma \in C^1(\mathbb{R}^2 \setminus \{\vec{0}\}, \mathbb{R}_{>0}) \cap C(\mathbb{R}^2, \mathbb{R}_{\geq 0})$ is a given anisotropy function. The function γ is positively homogeneous of degree one, i.e.

$$\gamma(\lambda\, \vec{p}) = \lambda\, \gamma(\vec{p}) \quad \forall\, \vec{p} \in \mathbb{R}^2,\ \forall\, \lambda \in \mathbb{R}_{\geq 0} \quad \Rightarrow \quad \gamma'(\vec{p})\,.\,\vec{p} = \gamma(\vec{p}) \quad \forall\, \vec{p} \in \mathbb{R}^2 \setminus \{\vec{0}\}, \tag{2.32}$$

where γ' is the gradient of γ. An anisotropy is called even, or absolutely homogeneous, if in addition to (2.32) it satisfies

$$\gamma(-\vec{p}) = \gamma(\vec{p}) \qquad \forall\, \vec{p} \in \mathbb{R}^2\,. \tag{2.33}$$

In the isotropic case we have that $\gamma(\vec{p}) = |\vec{p}|$ and so $\gamma(\vec{\nu}) = 1$, which means that $|\Gamma|_\gamma$ reduces to $|\Gamma|$, the surface area of Γ. A wide class of even anisotropies can be modelled by

$$\gamma(\vec{p}) = \sum_{\ell=1}^{L} \gamma^{(\ell)}(\vec{p}) = \sum_{\ell=1}^{L} \left[\vec{p}\,.\, G^{(\ell)}\,\vec{p}\right]^{\frac{1}{2}} \quad \Rightarrow \quad \gamma'(\vec{p}) = \sum_{\ell=1}^{L} [\gamma^{(\ell)}(\vec{p})]^{-1}\, G^{(\ell)}\,\vec{p} \quad \forall\ \vec{p} \in \mathbb{R}^2 \setminus \{\vec{0}\}, \tag{2.34}$$

where $G^{(\ell)} \in \mathbb{R}^{2\times 2}$, $\ell = 1 \to L$, are symmetric and positive definite. For the stability results in our previous papers on anisotropic evolution equations, see [13, 29–32, 37], we restricted ourselves to anisotropies of the form (2.34), as then it is possible to prove unconditional stability results for the fully discrete semi-implicit approximations introduced there. However, for the fully implicit approximations considered in this paper, it is possible to show stability for any smooth anisotropy that is convex. Indeed, the stability proof below will only make use of the estimate

$$\gamma'(\vec{p})\,.\,\vec{q} \leq \gamma(\vec{q}) \quad \forall\ \vec{p},\, \vec{q} \in \mathbb{R}^2 \setminus \{\vec{0}\}\,, \tag{2.35}$$

which, on recalling (2.32), is equivalent to $\gamma(\vec{p}) + \gamma'(\vec{p})\,.\,(\vec{q} - \vec{p}) \leq \gamma(\vec{q})$ for nontrivial $\vec{p},\, \vec{q} \in \mathbb{R}^2$, i.e. to γ being a smooth convex function on $\mathbb{R}^2 \setminus \{\vec{0}\}$. Of course, if γ is of the form (2.34), then it immediately follows from the Cauchy–Schwarz inequality that (2.35) holds.

The anisotropic curvature vector $\vec{\varkappa}_\gamma = \varkappa_\gamma\,\vec{\nu}$ is defined as the first variation of (2.31), see e.g. [1, 37] for details. In particular, the so called Cahn–Hoffmann vector, see [38], is defined by $\vec{\nu}_\gamma := \gamma'(\vec{\nu})$, where from now on we assume that $\vec{\nu} = -\vec{x}_s^{\,\perp}$ is the outer normal to Γ, with the weighted curvature given by

$$\varkappa_\gamma := -\vec{x}_s\,.\,(\vec{\nu}_\gamma)_s = -\vec{x}_s\,.\,[\gamma'(\vec{\nu})]_s\,. \tag{2.36}$$

Motion by anisotropic curvature and anisotropic surface diffusion are then given by

$$\text{(a)} \quad \mathcal{V} = \beta(\vec{\nu})\,\varkappa_\gamma \qquad \text{and} \qquad \text{(b)} \quad \mathcal{V} = -(\beta(\vec{\nu})\,[\varkappa_\gamma]_s)_s\,, \tag{2.37}$$

where $\beta : S^1 \to \mathbb{R}_{>0}$ is a given smooth and positive function, with $S^1 := \{\vec{p} \in \mathbb{R}^2 : |\vec{p}| = 1\}$ denoting the unit circle in $\mathbb{R}^2$. We recall that (2.37a,b) arise as weighted L^2- and H^{-1}-gradient flows of the anisotropic energy (2.31), respectively.

We then introduce the following fully discrete finite element approximations to (2.37a,b), where we note that (2.36) and (2.32) imply that $\varkappa_\gamma\,\vec{\nu} = [\gamma'(\vec{\nu})]_s^\perp \equiv [\gamma'(-\vec{x}_s^{\,\perp})]_s^\perp$. For $m \geq 0$, given $\vec{X}^m \in \underline{V}_0^h$, find $\Gamma^{m+1} = \vec{X}^{m+1}(I)$, with $\vec{X}^{m+1} \in \underline{V}_0^h$, and $\kappa_\gamma^{m+1} \in V_0^h$ such that

$$\begin{aligned} &\text{(a)} \\ &\text{(b)} \end{aligned} \quad \Big\langle \frac{\vec{X}^{m+1} - \vec{X}^m}{\tau_m}, \chi\,\vec{\nu}^{m+1} \Big\rangle^h_{\Gamma^{m+1}} - \begin{cases} \langle \beta(\vec{\nu}^{m+1})\,\kappa_\gamma^{m+1}, \chi \rangle^h_{\Gamma^{m+1}} \\ \langle \beta(\vec{\nu}^{m+1})\,[\kappa_\gamma^{m+1}]_s, \chi_s \rangle_{\Gamma^{m+1}} \end{cases} = 0 \quad \forall\ \chi \in V_0^h\,, \tag{2.38}$$

$$\langle \kappa_\gamma^{m+1}\,\vec{\nu}^{m+1}, \vec{\eta} \rangle^h_{\Gamma^{m+1}} - \langle \gamma'(\vec{\nu}^{m+1}), \vec{\eta}_s^{\,\perp} \rangle_{\Gamma^{m+1}} = 0 \quad \forall\ \vec{\eta} \in \underline{V}_0^h\,. \tag{2.39}$$

For later use we note that it follows from (2.32) that (2.39) can be equivalently written as

$$\langle \kappa_\gamma^{m+1}\,\vec{\nu}^{m+1}, \vec{\eta} \rangle^h_{\Gamma^{m+1}} + \langle \gamma(\vec{\nu}^{m+1})\,\vec{X}_s^{m+1}, \vec{\eta}_s \rangle_{\Gamma^{m+1}} = \langle \gamma'(\vec{\nu}^{m+1})\,.\,\vec{X}_s^{m+1}, \vec{\eta}_s\,.\,\vec{\nu}^{m+1} \rangle_{\Gamma^{m+1}} \quad \forall\ \vec{\eta} \in \underline{V}_0^h\,, \tag{2.40}$$

see e.g. [1] for details in the continuous case.

THEOREM. 2.7. *Let γ be such that it satisfies* (2.35)*, and let $(\vec{X}^m, \kappa_\gamma^m)_{m=1}^M$ be a solution of* (2.38a,b)*,* (2.39)*. Then for all $k = 1 \to M$ we have that*

$$\begin{array}{ll} \text{(a)} & |\Gamma^k|_\gamma + \sum_{m=0}^{k-1} \tau_m \begin{cases} \langle \beta(\vec{\nu}^{m+1})\, \kappa_\gamma^{m+1}, \kappa_\gamma^{m+1} \rangle_{\Gamma^{m+1}}^h \\ \langle \beta(\vec{\nu}^{m+1})\, [\kappa_\gamma^{m+1}]_s, [\kappa_\gamma^{m+1}]_s \rangle_{\Gamma^{m+1}} \end{cases} \leq |\Gamma^0|_\gamma \,, \\ \text{(b)} & \end{array} \tag{2.41}$$

where

$$|\Gamma^k|_\gamma = \int_{\Gamma^k} \gamma(\vec{\nu}^k)\, \mathrm{d}s = \int_I \gamma(-[\vec{X}_\rho^k]^\perp)\, \mathrm{d}\rho = \sum_{j=1}^J \gamma(-[\vec{h}_j^k]^\perp)\,. \tag{2.42}$$

Proof. Choosing $\chi = \kappa_\gamma^{m+1} \in V_0^h$ in (2.38a) and $\vec{\eta} = \frac{\vec{X}^{m+1} - \vec{X}^m}{\tau_m} \in \underline{V}_0^h$ in (2.39) yields that

$$-\langle \gamma'(\vec{\nu}^{m+1}), [\vec{X}_s^{m+1} - \vec{X}_s^m]^\perp \rangle_{\Gamma^{m+1}} + \tau_m \langle \beta(\vec{\nu}^{m+1})\, \kappa_\gamma^{m+1}, \kappa_\gamma^{m+1} \rangle_{\Gamma^{m+1}}^h = 0\,. \tag{2.43}$$

We now analyse the first term in (2.43). On recalling (2.3), (2.32) and (2.35), it holds that

$$\begin{aligned} -\langle \gamma'(\vec{\nu}^{m+1}), [\vec{X}_s^{m+1} - \vec{X}_s^m]^\perp \rangle_{\Gamma^{m+1}} &= -\int_{\Gamma^{m+1}} \gamma'(-[\vec{X}_s^{m+1}]^\perp) \,.\, [\vec{X}_s^{m+1} - \vec{X}_s^m]^\perp \,\mathrm{d}s \\ &= \sum_{j=1}^J \gamma'(-[\vec{h}_j^{m+1}]^\perp) \,.\, [-\vec{h}_j^{m+1} + \vec{h}_j^m]^\perp = \sum_{j=1}^J \gamma(-[\vec{h}_j^{m+1}]^\perp) + \gamma'(-[\vec{h}_j^{m+1}]^\perp) \,.\, [\vec{h}_j^m]^\perp \\ &\geq \sum_{j=1}^J \gamma(-[\vec{h}_j^{m+1}]^\perp) - \gamma(-[\vec{h}_j^m]^\perp) = |\Gamma^{m+1}|_\gamma - |\Gamma^m|_\gamma \,. \end{aligned} \tag{2.44}$$

Combining (2.43) and (2.44) yields that

$$|\Gamma^{m+1}|_\gamma - |\Gamma^m|_\gamma + \tau_m \langle \beta(\vec{\nu}^{m+1})\, \kappa_\gamma^{m+1}, \kappa_\gamma^{m+1} \rangle_{\Gamma^{m+1}}^h \leq 0\,. \tag{2.45}$$

Summing (2.45) for $m = 0 \to k-1$ yields the desired result (2.41a). The proof of (2.41b) is analogous. ∎

THEOREM. 2.8. *Let $(\vec{X}^{m+1}, \kappa_\gamma^{m+1})$ denote a solution to* (2.38a,b)*,* (2.39)*. Then it holds that*

$$\begin{aligned} \gamma(-[\vec{h}_j^{m+1}]^\perp) - \gamma(-[\vec{h}_{j-1}^{m+1}]^\perp) + \gamma'(-[\vec{h}_{j-1}^{m+1}]^\perp) \,.\, [\vec{h}_j^{m+1}]^\perp - \gamma'(-[\vec{h}_j^{m+1}]^\perp) \,.\, [\vec{h}_{j-1}^{m+1}]^\perp = 0\,, \\ \text{if} \quad \vec{h}_j^{m+1} \nparallel \vec{h}_{j-1}^{m+1}\,, \qquad j = 1 \to J\,. \end{aligned} \tag{2.46a}$$

If γ is of the form (2.34) *then* (2.46a) *implies that*

$$\sum_{\ell=1}^L \lambda_j^{m+1,\ell}\, \gamma^{(\ell)}([\vec{h}_j^{m+1}]^\perp) = \sum_{\ell=1}^L \lambda_j^{m+1,\ell}\, \gamma^{(\ell)}([\vec{h}_{j-1}^{m+1}]^\perp) \quad \text{if} \quad \vec{h}_j^{m+1} \nparallel \vec{h}_{j-1}^{m+1}\,, \qquad j = 1 \to J\,, \tag{2.46b}$$

where $\lambda_j^{m+1,\ell} := 1 - \frac{[\vec{h}_j^{m+1}]^\perp \,.\, G^{(\ell)}\,[\vec{h}_{j-1}^{m+1}]^\perp}{\gamma^{(\ell)}([\vec{h}_j^{m+1}]^\perp)\,\gamma^{(\ell)}([\vec{h}_{j-1}^{m+1}]^\perp)} \in [0,2]$, $\ell = 1 \to L$, $j = 1 \to J$; *with* $\lambda_j^{m+1,\ell} > 0$ *if* $\vec{h}_j^{m+1} \not\parallel \vec{h}_{j-1}^{m+1}$. *In the special case that* $L = 1$, *this yields that*

$$\gamma([\vec{h}_j^{m+1}]^\perp) = \gamma([\vec{h}_{j-1}^{m+1}]^\perp) \quad \textit{if} \quad \vec{h}_j^{m+1} \not\parallel \vec{h}_{j-1}^{m+1}\,, \qquad j = 1 \to J\,. \tag{2.46c}$$

Proof. The proof is analogous to the proof in [31, Remark 2.7] for the semidiscrete variant of (2.38b), (2.39). Fix an arbitrary $j \in \{1,\dots,J\}$. If $\vec{h}_j^{m+1} = \vec{0}$, $\vec{h}_{j-1}^{m+1} = \vec{0}$ or $\vec{h}_j^{m+1} + \vec{h}_{j-1}^{m+1} = \vec{0}$, then the claims (2.46a–c) trivially hold. In all the other cases we obtain, on choosing $\vec{\eta} = [\vec{\omega}^{m+1}(q_j)]^\perp\,\chi_j$ in (2.39), on recalling (2.2), and on noting that $[\vec{\omega}^{m+1}(q_j)]^\perp = \frac{\vec{h}_j^{m+1} + \vec{h}_{j-1}^{m+1}}{|\vec{h}_j^{m+1}| + |\vec{h}_{j-1}^{m+1}|}$, that

$$-\Big[\gamma'(-[\vec{h}_j^{m+1}]^\perp) - \gamma'(-[\vec{h}_{j-1}^{m+1}]^\perp)\Big]\,.\,\Big[\vec{h}_j^{m+1} + \vec{h}_{j-1}^{m+1}\Big]^\perp = 0\,, \tag{2.47}$$

and so (2.46a) holds. Moreover, if γ is of the form (2.34), it follows from (2.47) that $\sum_{\ell=1}^L \lambda_j^{m+1,\ell}\Big[\gamma^{(\ell)}([\vec{h}_j^{m+1}]^\perp) - \gamma^{(\ell)}([\vec{h}_{j-1}^{m+1}]^\perp)\Big] = 0$, i.e. that (2.46b) holds. Finally, (2.46c) follows immediately from (2.46b) on recalling that $\lambda_j^{m+1,\ell} > 0$ if $\vec{h}_j^{m+1} \not\parallel \vec{h}_{j-1}^{m+1}$. ∎

We observe that while only (2.46c) gives a rigorous result on the distribution of the vertices $\{\vec{X}^{m+1}(q_j)\}_{j=1}^J$ with respect to the anisotropy γ, nevertheless (2.46a) and (2.46b) also give certain conditions on the distribution of the mesh points. Unfortunately, it does not seem possible to derive stricter conditions for these more general anisotropies.

In view of the result (2.46c) for anisotropies of the form

$$\gamma(\vec{p}) = [\vec{p}\,.\,G\,\vec{p}]^{\frac{1}{2}}\,, \tag{2.48}$$

where $G \in \mathbb{R}^{2\times 2}$ is symmetric and positive definite, we introduce the following adaptation of the schemes (2.38a,b), (2.39) in the spirit of the isotropic schemes (2.16a,b), (2.17). For $m \geq 0$, given $\vec{X}^m \in \underline{V}_0^h$, find $\Gamma^{m+1} = \vec{X}^{m+1}(I)$, with $\vec{X}^{m+1} \in \underline{V}_0^h$, and $\kappa_\gamma^{m+1} \in V_0^h$ such that

$$\begin{array}{ll} \text{(a)} & \langle \dfrac{\vec{X}^{m+1} - \vec{X}^m}{\tau_m}, \chi\,\vec{\omega}^{m+1}\rangle_{\Gamma^{m+1}}^h - \begin{cases} \langle \beta(\vec{\nu}^{m+1})\,\kappa_\gamma^{m+1}, \chi\rangle_{\Gamma^{m+1}}^h \\ \langle \beta(\vec{\nu}^{m+1})\,[\kappa_\gamma^{m+1}]_s, \chi_s\rangle_{\Gamma^{m+1}} \end{cases} = 0 \quad \forall\ \chi \in V_0^h\,, \\ \text{(b)} & \end{array} \tag{2.49}$$

$$\langle \kappa_\gamma^{m+1}\,\vec{\omega}^{m+1}, \vec{\eta}\rangle_{\Gamma^{m+1}}^h + |\Gamma^{m+1}|_\gamma^{-1}\,\langle G\,[\vec{X}_\rho^{m+1}]^\perp, \vec{\eta}_\rho^{\,\perp}\rangle_I = 0 \quad \forall\ \vec{\eta} \in \underline{V}_0^h\,. \tag{2.50}$$

THEOREM. 2.9. *Let* γ *be of the form* (2.48). *Let* $(\vec{X}^m, \kappa_\gamma^m)_{m=1}^M$ *denote a solution to* (2.49,b), (2.50). *Then it holds that*

$$\gamma([\vec{h}_j^{m+1}]^\perp) = \gamma([\vec{h}_{j-1}^{m+1}]^\perp)\,, \qquad j = 1 \to J\,, \quad m = 0 \to M-1\,. \tag{2.51}$$

In addition, $(\vec{X}^m, \kappa_\gamma^m)_{m=1}^M$ *is a solution to* (2.38a,b), (2.39) *and, in particular, the stability results* (2.41a,b) *hold. Conversely, if* $(\vec{X}^{m+1}, \kappa_\gamma^{m+1})$ *is a solution to* (2.38a,b), (2.39) *such that* Γ^{m+1} *is truly equidistributed with respect to* γ, *then it also solves* (2.49a,b), (2.50).

Proof. Fix an arbitrary $j \in \{1, \dots, J\}$. If $\vec{\omega}^{m+1}(q_j) = \vec{0}$, then the claim (2.51) trivially holds. In all the other cases we obtain, on choosing $\vec{\eta} = [\vec{\omega}^{m+1}(q_j)]^\perp \, \chi_j$ in (2.50), that

$$0 = G\left(\vec{h}_j^{m+1} - \vec{h}_{j-1}^{m+1}\right)^\perp . \left(\vec{h}_j^{m+1} + \vec{h}_{j-1}^{m+1}\right)^\perp = \left(\gamma([\vec{h}_j^{m+1}]^\perp)\right)^2 - \left(\gamma([\vec{h}_{j-1}^{m+1}]^\perp)\right)^2 .$$

This proves (2.51). The remaining claims then follow on noting that (2.51), (2.42), (2.48) and (2.1) imply that

$$\begin{aligned} |\Gamma^{m+1}|_\gamma^{-1} \, \langle G\,[\vec{X}_\rho^{m+1}]^\perp, \vec{\eta}_\rho^{\,\perp} \rangle_I &= \int_I \frac{G\,[\vec{X}_\rho^{m+1}]^\perp \,.\, \vec{\eta}_\rho^{\,\perp}}{\gamma([\vec{X}_\rho^{m+1}]^\perp)} \,\mathrm{d}\rho = \langle [\gamma(\vec{\nu}^{m+1})]^{-1} \, G\,[\vec{X}_s^{m+1}]^\perp, \vec{\eta}_s^{\,\perp} \rangle_{\Gamma^{m+1}} \\ &= \langle \gamma'([\vec{X}_s^{m+1}]^\perp), \vec{\eta}_s^{\,\perp} \rangle_{\Gamma^{m+1}} = -\langle \gamma'(\vec{\nu}^{m+1}), \vec{\eta}_s^{\,\perp} \rangle_{\Gamma^{m+1}} \qquad \forall\ \vec{\eta} \in \underline{V}_0^h \,. \end{aligned}$$

□

If we assume that $\gamma \in C^2(\mathbb{R}^2 \setminus \{\vec{0}\}, \mathbb{R}_{>0})$, then the following approximation of (2.37a) can also be considered. Here we recall from [6] that

$$\varkappa_\gamma = a(\vec{\nu})\, \varkappa \,, \quad \text{where} \quad a(\vec{\nu}) \equiv a(-\vec{x}_s^{\,\perp}) := \gamma''(-\vec{x}_s^{\,\perp})\, \vec{x}_s \,.\, \vec{x}_s \,, \tag{2.52}$$

where γ'' denotes the Hessian of γ, and where we recall for later use that

$$\gamma''(\vec{p})\, \vec{p} = \vec{0} \quad \forall\ \vec{p} \in S^1 \,. \tag{2.53}$$

A common formulation of (2.52) uses the identity $a(\vec{\nu}) = \widehat{\gamma}''(\theta) + \widehat{\gamma}(\theta)$, where $\widehat{\gamma}(\theta) := \gamma(\cos\theta, \sin\theta) = \gamma(\vec{\nu})$ and θ is the angle that $\vec{\nu}$ makes with the x_1-axis; see e.g. [39]. Hence (2.37a,b) can be rewritten as

$$\text{(a)} \quad \mathcal{V} = \beta(\vec{\nu})\, a(\vec{\nu})\, \varkappa \qquad \text{and} \qquad \text{(b)} \quad \mathcal{V} = -(\beta(\vec{\nu})\, [a(\vec{\nu})\, \varkappa]_s)_s \,, \tag{2.54}$$

and it is not difficult to show that (2.54a) implies that

$$\frac{\mathrm{d}}{\mathrm{d}t} \, |\Gamma(t)| = -\int_{\Gamma(t)} \beta(\vec{\nu})\, a(\vec{\nu})\, \varkappa^2 \,\mathrm{d}s \,, \tag{2.55}$$

i.e. (2.54a) can also be viewed as a weighted L^2-gradient flow of the isotropic length (1.4). We propose the following approximation to (2.54a). For $m \geq 0$, given $\vec{X}^m \in \underline{V}_0^h$, find $\Gamma^{m+1} = \vec{X}^{m+1}(I)$, with $\vec{X}^{m+1} \in \underline{V}_0^h$, and $\kappa^{m+1} \in V_0^h$ such that

$$\left\langle \frac{\vec{X}^{m+1} - \vec{X}^m}{\tau_m}, \chi\, \vec{\nu}^{m+1} \right\rangle_{\Gamma^{m+1}}^h - \langle \beta(\vec{\nu}^{m+1})\, a(\vec{\nu}^{m+1})\, \kappa^{m+1}, \chi \rangle_{\Gamma^{m+1}}^h = 0 \qquad \forall\ \chi \in V_0^h \,, \tag{2.56a}$$

$$\langle \kappa^{m+1}\, \vec{\nu}^{m+1}, \vec{\eta} \rangle_{\Gamma^{m+1}}^h + \langle \vec{X}_s^{m+1}, \vec{\eta}_s \rangle_{\Gamma^{m+1}} = 0 \qquad \forall\ \vec{\eta} \in \underline{V}_0^h \,. \tag{2.56b}$$

On assuming that

$$a(\vec{p}) \geq 0 \qquad \forall\ \vec{p} \in S^1 \,, \tag{2.57}$$

which on recalling (2.53) is equivalent to $\gamma''(\vec{p})$ being positive semidefinite for all $\vec{p} \in S^1$, i.e. equivalent to γ being convex, it is easy for (2.56a,b) to establish the stability result (2.10a) with the terms in the sum replaced by $\tau_m \, \langle \beta(\vec{\nu}^{m+1})\, a(\vec{\nu}^{m+1})\, \kappa^{m+1}, \kappa^{m+1} \rangle_{\Gamma^{m+1}}^h$. This

is a discrete analogue of (2.55). Moreover, a solution to (2.56a,b) will satisfy Theorem 2.2, i.e. the curves Γ^{m+1}, $m = 0 \to M-1$, will be equidistributed where they are not locally flat. Hence the reformulation (2.56a) with (2.17) can also be considered, and the obvious analogue of Theorem 2.3 then holds for this new approximation. We stress that the equidistribution here is with respect to the isotropic length, and so is very different to the results in Theorem 2.8 and Theorem 2.9.

For corresponding approximations of (2.54b) no stability can be expected. However, for the interested reader we state a fully discrete, fully implicit approximation of (2.54b) for completeness. Here we assume strict positivity in (2.57). For $m \geq 0$, given $\vec{X}^m \in \underline{V}_0^h$, find $\Gamma^{m+1} = \vec{X}^{m+1}(I)$, with $\vec{X}^{m+1} \in \underline{V}_0^h$, and $\kappa_\gamma^{m+1} \in V_0^h$ such that

$$\langle \frac{\vec{X}^{m+1} - \vec{X}^m}{\tau_m}, \chi\, \vec{\nu}^{m+1} \rangle^h_{\Gamma^{m+1}} - \langle \beta(\vec{\nu}^{m+1})\, [\kappa_\gamma^{m+1}]_s, \chi_s \rangle_{\Gamma^{m+1}} = 0 \qquad \forall\ \chi \in V_0^h\,, \tag{2.58a}$$

$$\langle \tilde{a}^{m+1}\, \kappa_\gamma^{m+1}\, \vec{\nu}^{m+1}, \vec{\eta} \rangle^h_{\Gamma^{m+1}} + \langle \vec{X}_s^{m+1}, \vec{\eta}_s \rangle_{\Gamma^{m+1}} = 0 \qquad \forall\ \vec{\eta} \in \underline{V}_0^h\,, \tag{2.58b}$$

where $\tilde{a}^{m+1} \in V_0^h$ is defined by

$$\tilde{a}^{m+1}(q_j) := \tfrac{1}{2} \left([a(\vec{\nu}_j^{m+1})]^{-1} + [a(\vec{\nu}_{j-1}^{m+1})]^{-1} \right), \quad \text{with} \quad \vec{\nu}_j^{m+1} := \frac{-[\vec{h}_j^{m+1}]^\perp}{|\vec{h}_j^{m+1}|}\,,$$

for $j = 1 \to J$. As before, it is easy to show that a solution to (2.58a,b) will satisfy Theorem 2.2. Moreover, on replacing (2.58b) with

$$\langle \tilde{a}^{m+1}\, \kappa_\gamma^{m+1}\, \vec{\nu}^{m+1}, \vec{\eta} \rangle^h_{\Gamma^{m+1}} + |\Gamma^{m+1}|^{-1}\, \langle \vec{X}_\rho^{m+1}, \vec{\eta}_\rho \rangle_I = 0 \qquad \forall\ \vec{\eta} \in \underline{V}_0^h\,, \tag{2.59}$$

true equidistribution as in Theorem 2.3 can be shown. Obviously, replacing $\tilde{a}^{m+1}$ in (2.58b) with $[a(\vec{\nu}^{m+1})]^{-1}$ gives an alternative approximation of (2.54b) that will no longer satisfy Theorem 2.2.

REMARK. 2.5. *It is worthwhile to consider the following semi-implicit variant of* (2.56a,b). *For $m \geq 0$, given $\Gamma^m = \vec{X}^m(I)$, with $\vec{X}^m \in \underline{V}_0^h$, find $\Gamma^{m+1} = \vec{X}^{m+1}(I)$, with $\vec{X}^{m+1} \in \underline{V}_0^h$, and $\kappa^{m+1} \in V_0^h$ such that*

$$\langle \frac{\vec{X}^{m+1} - \vec{X}^m}{\tau_m}, \chi\, \vec{\nu}^m \rangle^h_{\Gamma^m} - \langle \beta(\vec{\nu}^m)\, a(\vec{\nu}^m)\, \kappa^{m+1}, \chi \rangle^h_{\Gamma^m} = 0 \quad \forall\ \chi \in V_0^h \quad \text{and} \quad (2.8). \tag{2.60}$$

Using the techniques in [12,31], and on assuming some mild assumptions on Γ^m, it is then not difficult to establish existence and uniqueness for the linear system (2.60). *Moreover, it is straightforward to show that $|\Gamma^{m+1}| + \tau_m\, \langle \beta(\vec{\nu}^m)\, a(\vec{\nu}^m)\, \kappa^{m+1}, \kappa^{m+1} \rangle^h_{\Gamma^m} \leq |\Gamma^m|$, i.e. a discrete analogue of* (2.55) *holds, which for anisotropies satisfying* (2.57) *yields unconditional stability. A disadvantage of* (2.60) *over previous semi-implicit approximations of* (2.37a) *introduced by the authors in e.g. [13,31] is that it does not appear possible to show that the weighted length $|\Gamma^m|_\gamma$ is decreased over each time step, and so the anisotropic gradient flow structure of* (2.37a) *is not mimicked on the discrete level. An advantage of* (2.60), *on the other hand, is that more general anisotropies than of the form* (2.34) *can be considered. E.g. in* Section 4 *we will show evolutions for* (2.60) *for anisotropies with*

triangular and pentagonal Wulff shapes, which means that for these anisotropies (2.33) *does not hold. Similarly, the natural semi-implicit variant of* (2.58a,b) *can also be considered. But due to the lack of a stability result, this particular approximation is not of much interest.*

2.3 Other situations

One can also introduce fully implicit variants of the semi-implicit approximations introduced in [13] for gradient flows of (1.4) for $\vec{x}(t) : I \to \mathbb{R}^d$, $d \geq 2$; i.e. for curve evolutions in higher codimensions. The same is true for fully implicit finite element approximations of geodesic flows, which arise as gradient flows of e.g. (1.4), when the curve is restricted to lie on a two-dimensional manifold $\mathcal{M} \subset \mathbb{R}^3$. Although the ideas presented in this paper carry across to these higher codimension flows, the finite element approximations will be slightly more involved due to the solution-dependent test and trial spaces introduced in [13]. We will report on these issues in more detail elsewhere. Similarly, fully implicit schemes based on the approximations in [11, 13] can be obtained for the elastic flow of curves, where the energy (1.4) is replaced by $E(\Gamma(t)) = \int_{\Gamma(t)} |\vec{\varkappa}|^2 \,\mathrm{d}s$, recall (1.2). Moreover, nonlinear curve shortening flows in the plane of the form $\mathcal{V} = f(\varkappa)$, where $f : (a, b) \to \mathbb{R}$, with $-\infty \leq a < b \leq \infty$, is a strictly monotonically increasing continuous function, can also be considered. The relevant details for the semi-implicit schemes can be found in [12]. Finally, fully implicit finite element approximations for the evolution of phase boundaries in solidification processes, modelled by e.g. Stefan problems or Mullins–Sekerka problems, can be obtained on generalizing the semi-implicit approximations introduced in [32].

In each case, the fully implicit scheme will share the equidistribution properties highlighted in Theorems 2.2 and 2.3 for isotropic evolutions, and Theorems 2.8 and 2.9 in anisotropic situations. In addition, where the semi-implicit scheme satisfies a stability property, an analogous stability result will hold for the fully implicit approximation.

3 Solution of the algebraic equations

In order to find solutions to the schemes (2.4a,b), (2.5), we employ the following iterative solution method. At each time step, given $\Gamma^{m+1,0} = \vec{X}^{m+1,0}(I)$, we seek for $i \geq 0$ solutions $(\vec{X}^{m+1,i+1}, \kappa^{m+1,i+1}) \in \underline{V}_0^h \times V_0^h$ such that

$$\text{(a)} \quad \text{(b)} \qquad \Big\langle \frac{\vec{X}^{m+1,i+1} - \vec{X}^{m}}{\tau_m}, \chi\, \vec{\omega}^{m+1,i} \Big\rangle^h_{\Gamma^{m+1,i}} - \begin{cases} \langle \kappa^{m+1,i+1}, \chi \rangle^h_{\Gamma^{m+1,i}} \\ \langle \kappa_s^{m+1,i+1}, \chi_s \rangle_{\Gamma^{m+1,i}} \end{cases} = 0 \quad \forall\ \chi \in V_0^h, \tag{3.1}$$

$$\langle \kappa^{m+1,i+1}\, \vec{\omega}^{m+1,i}, \vec{\eta} \rangle^h_{\Gamma^{m+1,i}} + \langle \vec{X}_s^{m+1,i+1}, \vec{\eta}_s \rangle_{\Gamma^{m+1,i}} = 0 \quad \forall\ \vec{\eta} \in \underline{V}_0^h\,. \tag{3.2}$$

Note that now, crucially, (3.1a,b), (3.2) are linear systems. Existence and uniqueness to (3.1a,b), (3.2) is equivalent to existence and uniqueness to (2.7a,b), (2.8), and the latter was shown in [11, 12] under some mild assumptions on Γ^m. The iterations (3.1a,b), (3.2) are repeated until $\|\vec{X}^{m+1,i+1} - \vec{X}^{m+1,i}\|_\infty < \mathrm{tol}$, where $\mathrm{tol} = 10^{-8}$ is a chosen tolerance. In

practice, the iterations (3.1a,b), (3.2) always converged if the curve $\Gamma^{m+1,0}$ was sufficiently close to being equidistributed. Of course, we always set $\Gamma^{m+1,0} = \Gamma^m$, which for $m > 0$ is equidistributed. Hence only for the first time step care needs to be taken in the choice of Γ^0.

On recalling Theorem 2.3, an alternative solution procedure for the schemes (2.4a,b), (2.5), which in fact finds a solution to (2.16a,b), (2.17), is the following iteration. At each time step, given $\Gamma^{m+1,0} = \vec{X}^{m+1,0}(I)$, we seek for $i \geq 0$ solutions $(\vec{X}^{m+1,i+1}, \kappa^{m+1,i+1}) \in \underline{V}_0^h \times V_0^h$ such that

$$\text{(a)} \quad \text{(b)} \quad \langle \frac{\vec{X}^{m+1,i+1} - \vec{X}^m}{\tau_m}, \chi\,(\vec{X}_\rho^{m+1,i})^\perp \rangle_I^h + \begin{cases} |\Gamma^{m+1,i}|\,\langle \kappa^{m+1,i+1}, \chi \rangle_I^h \\ |\Gamma^{m+1,i}|^{-1}\,\langle \kappa_\rho^{m+1,i+1}, \chi_\rho \rangle_I \end{cases} = 0 \quad \forall\ \chi \in V_0^h, \tag{3.3}$$

$$\langle \kappa^{m+1,i+1}\,(\vec{X}_\rho^{m+1,i})^\perp, \vec{\eta} \rangle_I^h - |\Gamma^{m+1,i}|^{-1}\,\langle \vec{X}_\rho^{m+1,i+1}, \vec{\eta}_\rho \rangle_I = 0 \quad \forall\ \vec{\eta} \in \underline{V}_0^h\,. \tag{3.4}$$

Once again we observe that (3.3a,b), (3.4) are linear systems. Existence and uniqueness of a solution to (3.3a,b), (3.4) can be shown similarly to (3.1a,b), (3.2). We remark that as the reformulations (2.16a,b), (2.17) of (2.4a,b), (2.5), on which the iterations (3.3a,b), (3.4) are based, are much less nonlinear than (2.4a,b), (2.5), we would expect the iterations (3.3a,b), (3.4) to perform better in practice than the iterations (3.1a,b), (3.2). This is indeed what can be observed in practice, where we see that the former iterations are a number of magnitudes faster than the latter. But as noted previously, also the iterations (3.3a,b), (3.4) will only converge if $\Gamma^{m+1,0}$ is sufficiently close to being equidistributed. In practice, we will always choose $\Gamma^{m+1,0} = \Gamma^m$, with Γ^0 being an equidistributed polygonal approximation of $\Gamma(0)$. Then the iterations (3.3a,b), (3.4) always converged in less than ten steps. Hence for all of the results in Section 4 for the approximations (2.4a,b), (2.5) we will employ the iterations (3.3a,b), (3.4) unless otherwise stated.

REMARK. 3.1. *As an alternative solution method, it is worthwhile to consider Newton's method. With a view towards possibly using Newton's method for the general anisotropic schemes* (2.38a,b), (2.39)*, we first consider the much simpler approximation* (2.4a), (2.5)*. Denoting that nonlinear system formally by* $F(\vec{X}^{m+1}, \kappa^{m+1}) = 0$ *for a nonlinear function* $F : \mathbb{R}^{3J} \to \mathbb{R}^{3J}$*, we can compute the first variation of* F *at the point* $(\vec{X}^{m+1}, \kappa^{m+1})$ *in a direction* $(\vec{\xi}, \phi)$*. Then, given* $(\vec{X}^{m+1,i}, \kappa^{m+1,i})$*, the solution of a Newton step*

$$F'(\vec{X}^{m+1,i}, \kappa^{m+1,i})\,(\vec{\xi}, \phi) = -F(\vec{X}^{m+1,i}, \kappa^{m+1,i})\,, \tag{3.5}$$

with $\vec{X}^{m+1,i+1} := \vec{X}^{m+1,i} + \vec{\xi}$*,* $\kappa^{m+1,i+1} := \kappa^{m+1,i} + \phi$*, can be found as follows. Find* $(\vec{\xi}, \phi) \in \underline{V}_0^h \times V_0^h$ *such that*

$$\begin{aligned} &\langle \frac{\vec{\xi}}{\tau_m} \cdot \vec{\omega}^{m+1,i} - \frac{\vec{X}^{m+1,i} - \vec{X}^m}{\tau_m} \cdot \vec{\xi}_s^{\,\perp}, \chi \rangle_{\Gamma^{m+1,i}}^h - \langle \phi, \chi \rangle_{\Gamma^{m+1,i}}^h - \langle \kappa^{m+1,i}\,\vec{X}_s^{m+1,i} \cdot \vec{\xi}_s, \chi \rangle_{\Gamma^{m+1,i}}^h \\ &\qquad = -\langle \frac{\vec{X}^{m+1,i} - \vec{X}^m}{\tau_m}, \chi\,\vec{\omega}^{m+1,i} \rangle_{\Gamma^{m+1,i}}^h + \langle \kappa^{m+1,i}, \chi \rangle_{\Gamma^{m+1,i}}^h \qquad \forall\ \chi \in V_0^h, \end{aligned} \tag{3.6a}$$

$$\begin{aligned} &\langle \phi\,\vec{\omega}^{m+1,i}, \vec{\eta} \rangle_{\Gamma^{m+1,i}}^h - \langle \kappa^{m+1,i}\,\vec{\xi}_s^{\,\perp}, \vec{\eta} \rangle_{\Gamma^{m+1,i}}^h + \langle (\vec{Id} - \vec{X}_s^{m+1,i} \otimes \vec{X}_s^{m+1,i})\,\vec{\xi}_s, \vec{\eta}_s \rangle_{\Gamma^{m+1,i}} \\ &\qquad = -\langle \kappa^{m+1,i}\,\vec{\omega}^{m+1,i}, \vec{\eta} \rangle_{\Gamma^{m+1,i}}^h - \langle \vec{X}_s^{m+1,i}, \vec{\eta}_s \rangle_{\Gamma^{m+1,i}} \qquad \forall\ \vec{\eta} \in \underline{V}_0^h\,. \end{aligned} \tag{3.6b}$$

The variable ϕ can be eliminated from the above system to yield the following reduced equation. Find $\vec{\xi} \in \underline{V}_0^h$ such that

$$\begin{aligned}\langle \frac{\vec{\xi}}{\tau_m} \,.\, \vec{\omega}^{m+1,i} - \frac{\vec{X}^{m+1,i} - \vec{X}^m}{\tau_m} \,.\, \vec{\xi}_s^{\perp}, \vec{\eta} \,.\, \vec{\omega}^{m+1,i} \rangle^h_{\Gamma^{m+1,i}} - \langle \kappa^{m+1,i}\, \vec{X}_s^{m+1,i} \,.\, \vec{\xi}_s, \vec{\eta} \,.\, \vec{\omega}^{m+1,i} \rangle^h_{\Gamma^{m+1,i}} \\ - \langle \kappa^{m+1,i}\, \vec{\xi}_s^{\perp}, \vec{\eta} \rangle^h_{\Gamma^{m+1,i}} + \langle (\vec{Id} - \vec{X}_s^{m+1,i} \otimes \vec{X}_s^{m+1,i})\, \vec{\xi}_s, \vec{\eta}_s \rangle_{\Gamma^{m+1,i}} \\ = -\langle \frac{\vec{X}^{m+1,i} - \vec{X}^m}{\tau_m} \,.\, \vec{\omega}^{m+1,i}, \vec{\eta} \,.\, \vec{\omega}^{m+1,i} \rangle^h_{\Gamma^{m+1,i}} - \langle \vec{X}_s^{m+1,i}, \vec{\eta}_s \rangle_{\Gamma^{m+1,i}} \qquad \forall\ \vec{\eta} \in \underline{V}_0^h \,. \quad (3.7)\end{aligned}$$

Unfortunately, the system (3.7)*, and hence* (3.6a,b)*, can become singular in practice, and this is e.g. observed when $\Gamma^{m+1,i}$ contains locally parallel elements. Considering a generalized Newton's method as described in e.g. [40] did not overcome this problem.*

For the sake of completeness, we note that a similar calculation for the nonlinear system (2.4b)*,* (2.5) *yields that the update for the Newton step* (3.5)*, now for the scheme* (2.4b)*,* (2.5)*, is given by the following solution. Find $(\vec{\xi}, \phi) \in \underline{V}_0^h \times V_0^h$ such that*

$$\begin{aligned}\langle \frac{\vec{\xi}}{\tau_m} \,.\, \vec{\omega}^{m+1,i} - \frac{\vec{X}^{m+1,i} - \vec{X}^m}{\tau_m} \,.\, \vec{\xi}_s^{\perp}, \chi \rangle^h_{\Gamma^{m+1,i}} - \langle \phi_s, \chi_s \rangle_{\Gamma^{m+1,i}} + \langle \kappa_s^{m+1,i}\, \vec{X}_s^{m+1,i} \,.\, \vec{\xi}_s, \chi_s \rangle_{\Gamma^{m+1,i}} \\ = -\langle \frac{\vec{X}^{m+1,i} - \vec{X}^m}{\tau_m}, \chi\, \vec{\omega}^{m+1,i} \rangle^h_{\Gamma^{m+1,i}} + \langle \kappa_s^{m+1,i}, \chi_s \rangle_{\Gamma^{m+1,i}} \qquad \forall\ \chi \in V_0^h, \quad (3.8a)\end{aligned}$$

$$\begin{aligned}\langle \phi\, \vec{\omega}^{m+1,i}, \vec{\eta} \rangle^h_{\Gamma^{m+1,i}} - \langle \kappa^{m+1,i}\, \vec{\xi}_s^{\perp}, \vec{\eta} \rangle^h_{\Gamma^{m+1,i}} + \langle (\vec{Id} - \vec{X}_s^{m+1,i} \otimes \vec{X}_s^{m+1,i})\, \vec{\xi}_s, \vec{\eta}_s \rangle_{\Gamma^{m+1,i}} \\ = -\langle \kappa^{m+1,i}\, \vec{\omega}^{m+1,i}, \vec{\eta} \rangle^h_{\Gamma^{m+1,i}} - \langle \vec{X}_s^{m+1,i}, \vec{\eta}_s \rangle_{\Gamma^{m+1,i}} \qquad \forall\ \vec{\eta} \in \underline{V}_0^h \,. \quad (3.8b)\end{aligned}$$

On the other hand, writing the nonlinear system (2.9) *formally as $G(\vec{X}^{m+1}) = 0$ for a nonlinear function $G : \mathbb{R}^{2J} \to \mathbb{R}^{2J}$, we can compute the first variation of G at the point $\vec{X}^{m+1}$ in a direction $\vec{\xi}$. Then, given $\vec{X}^{m+1,i}$, the solution of a Newton step $G'(\vec{X}^{m+1,i})\, \vec{\xi} = -G(\vec{X}^{m+1,i})$, with $\vec{X}^{m+1,i+1} := \vec{X}^{m+1,i} + \vec{\xi}$, can be found as follows. Find $\vec{\xi} \in \underline{V}_0^h$ such that*

$$\begin{aligned}\langle \frac{\vec{\xi}}{\tau_m} + \frac{\vec{X}^{m+1,i} - \vec{X}^m}{\tau_m}\, \vec{\xi}_s \,.\, \vec{X}_s^{m+1,i}, \vec{\eta} \rangle^h_{\Gamma^{m+1,i}} + \langle (\vec{Id} - \vec{X}_s^{m+1,i} \otimes \vec{X}_s^{m+1,i})\, \vec{\xi}_s, \vec{\eta}_s \rangle_{\Gamma^{m+1,i}} \\ = -\langle \frac{\vec{X}^{m+1,i} - \vec{X}^m}{\tau_m}, \vec{\eta} \rangle^h_{\Gamma^{m+1,i}} - \langle \vec{X}_s^{m+1,i}, \vec{\eta}_s \rangle_{\Gamma^{m+1,i}} \qquad \forall\ \vec{\eta} \in \underline{V}_0^h \,. \quad (3.9)\end{aligned}$$

We note that (3.9) *will in general be nonsingular, and in fact will be well conditioned, due to the presence of the mass matrix contribution $\frac{1}{\tau_m} \langle \vec{\xi}, \vec{\eta} \rangle^h_{\Gamma^{m+1,i}}$. This is in contrast to* (3.7)*, where no such good conditioning can be expected, and where singular systems may be encountered during the iteration. In practice we observe that the Newton iteration* (3.9) *always converges for the initial guess $\vec{X}^{m+1,0} = \vec{X}^m$ if τ_m is chosen sufficiently small.*

3.1 Curve Networks

Naturally, the iterations (3.3a,b), (3.4) can easily be generalized to the approximations (2.28a,b), (2.29) so that they find solutions to the schemes (2.24a,b), (2.25). As this is straightforward, we omit the details.

3.2 Anisotropic surface energies

In order to find solutions to the schemes (2.38a,b), (2.39) we employ the following iterative solution method, where we recall (2.40). At each time step, given $\Gamma^{m+1,0} = \vec{X}^{m+1,0}(I)$, we seek for $i \geq 0$ solutions $(\vec{X}^{m+1,i+1}, \kappa_\gamma^{m+1,i+1}) \in \underline{V}_0^h \times V_0^h$ such that

$$\begin{array}{ll} \text{(a)} \\ \text{(b)} \end{array} \quad \langle \frac{\vec{X}^{m+1,i+1} - \vec{X}^m}{\tau_m}, \chi\, \vec{\omega}^{m+1,i} \rangle^h_{\Gamma^{m+1,i}} - \begin{cases} \langle \beta(\vec{\nu}^{m+1,i})\, \kappa_\gamma^{m+1,i+1}, \chi \rangle^h_{\Gamma^{m+1,i}} \\ \langle \beta(\vec{\nu}^{m+1,i})\, [\kappa_\gamma^{m+1,i+1}]_s, \chi_s \rangle_{\Gamma^{m+1,i}} \end{cases} = 0 \quad \forall\, \chi \in V_0^h, \tag{3.10}$$

$$\langle \kappa_\gamma^{m+1,i+1}\, \vec{\omega}^{m+1,i}, \vec{\eta} \rangle^h_{\Gamma^{m+1,i}} + \langle \gamma(\vec{\nu}^{m+1,i})\, \vec{X}_s^{m+1,i+1}, \vec{\eta}_s \rangle_{\Gamma^{m+1,i}} = \langle \gamma'(\vec{\nu}^{m+1,i})\,.\, \vec{X}_s^{m+1,i}, \vec{\eta}_s\,.\, \vec{\nu}^{m+1,i} \rangle_{\Gamma^{m+1,i}} \quad \forall\, \vec{\eta} \in \underline{V}_0^h\,. \tag{3.11}$$

If the anisotropy γ is of the form (2.34), then the following iterations, which are based on the semi-implicit schemes introduced in [31], can also be employed. At each time step, given $\Gamma^{m+1,0} = \vec{X}^{m+1,0}(I)$, we seek for $i \geq 0$ solutions $(\vec{X}^{m+1,i+1}, \kappa_\gamma^{m+1,i+1}) \in \underline{V}_0^h \times V_0^h$ such that

$$\langle \kappa_\gamma^{m+1,i+1}\, \vec{\omega}^{m+1,i}, \vec{\eta} \rangle^h_{\Gamma^{m+1,i}} + \sum_{\ell=1}^{L} \langle [\gamma^{(\ell)}(\vec{\nu}^{m+1,i})]^{-1}\, G^{(\ell)}\, [\vec{X}_s^{m+1,i+1}]^\perp, \vec{\eta}_s^{\,\perp} \rangle_{\Gamma^{m+1,i}} = 0 \quad \forall\, \vec{\eta} \in \underline{V}_0^h \text{ and (a) (3.10a), or (b) (3.10b).} \tag{3.12}$$

For later use, we also define the following semi-implicit approximation of the flow $\mathcal{V} = 0$, which is the natural anisotropic analogue of [11, (2.23a,b)]. Given $\Gamma^0 = \vec{X}^0(I)$, for $m = 0 \to M-1$ find $(\vec{X}^{m+1}, \kappa_\gamma^{m+1}) \in \underline{V}_0^h \times V_0^h$ such that

$$\langle \vec{X}^{m+1} - \vec{X}^m, \chi\, \vec{\omega}^m \rangle^h_{\Gamma^m} = 0 \qquad \forall\, \chi \in V_0^h, \tag{3.13a}$$

$$\langle \kappa_\gamma^{m+1}\, \vec{\omega}^m, \vec{\eta} \rangle^h_{\Gamma^m} + \sum_{\ell=1}^{L} \langle [\gamma^{(\ell)}(\vec{\nu}^m)]^{-1}\, G^{(\ell)}\, [\vec{X}_s^{m+1}]^\perp, \vec{\eta}_s^{\,\perp} \rangle_{\Gamma^m} = 0 \qquad \forall\, \vec{\eta} \in \underline{V}_0^h\,. \tag{3.13b}$$

In Section 4, the scheme (3.13a,b) will be employed in order to obtain a discretization Γ^0 of $\Gamma(0)$, which is very close to satisfying (2.46b). Moreover, on recalling Theorem 2.9, an alternative solution procedure for the schemes (2.38a,b), (2.39) in the case that γ is of the form (2.48), which in fact finds a solution to (2.49a,b), (2.50) is the following iteration. At each time step, given $\Gamma^{m+1,0} = \vec{X}^{m+1,0}(I)$, we seek for $i \geq 0$ solutions $(\vec{X}^{m+1,i+1}, \kappa_\gamma^{m+1,i+1}) \in \underline{V}_0^h \times V_0^h$ such that

$$\langle \kappa_\gamma^{m+1,i+1}\, \vec{\omega}^{m+1,i}, \vec{\eta} \rangle^h_{\Gamma^{m+1,i}} + |\Gamma^{m+1,i}|_\gamma^{-1}\, \langle G\, [\vec{X}_\rho^{m+1,i+1}]^\perp, \vec{\eta}_\rho^{\,\perp} \rangle_I = 0 \qquad \forall\, \vec{\eta} \in \underline{V}_0^h \text{ and (a) (3.10a), or (b) (3.10b).} \tag{3.14}$$

Finally, a solution method for the scheme (2.56a,b), which in fact finds a solution to the reformulation (2.56a), (2.17), is the following iteration. At each time step, given $\Gamma^{m+1,0} = \vec{X}^{m+1,0}(I)$, we seek for $i \geq 0$ solutions $(\vec{X}^{m+1,i+1}, \kappa^{m+1,i+1}) \in \underline{V}_0^h \times V_0^h$ such that

$$\langle \frac{\vec{X}^{m+1,i+1} - \vec{X}^m}{\tau_m}, \chi\, (\vec{X}_\rho^{m+1,i})^\perp \rangle^h_I + |\Gamma^{m+1,i}|\, \langle \beta(\vec{\nu}^{m+1,i})\, a(\vec{\nu}^{m+1,i})\, \kappa^{m+1,i+1}, \chi \rangle^h_I = 0\,, \tag{3.15}$$

J	(2.4a), (2.5)	eoc	(2.7a), (2.8)	eoc
256	1.2713e-04	–	1.6794e-04	–
512	3.1768e-05	2.000658	4.2031e-05	1.998420
1024	7.9410e-06	2.000182	1.0511e-05	1.999554
2048	1.9852e-06	2.000036	2.6279e-06	1.999918

Table 1: Absolute errors $\|\vec{X} - \vec{x}\|_{L^\infty}$ and experimental orders of convergence (eoc).

for all $\chi \in V_0^h$, and (3.4) hold. Analogously an iteration for the scheme (2.58a,b), which finds a solution to (2.58a), (2.59), can be formulated.

4 Numerical Results

Throughout this section we use (almost) uniform time steps; in that, $\tau_m = \tau$, $m = 0 \to M-2$, and $\tau_{M-1} = T - t_{M-1} \leq \tau$. For later purposes, we define $\vec{X}(t) := \frac{t-t_{m-1}}{\tau}\,\vec{X}^m + \frac{t_m - t}{\tau}\,\vec{X}^{m-1}$, $t \in [t_{m-1}, t_m]$, $m \geq 1$. In this section we will often compare numerical results from the fully implicit finite element approximations introduced in this paper with results from the appropriate semi-implicit approximations. Where these results are graphically indistinguishable, we will only show the results for the fully implicit schemes.

An exact solution to (1.8a), (1.9) is given by the shrinking circles

$$\vec{x}(\rho,t) = (1-2\,t)^{\frac{1}{2}}\,(\cos 2\,\pi\,\rho, \sin 2\,\pi\,\rho)^T, \quad \varkappa(\rho,t) = (1-2\,t)^{-\frac{1}{2}}, \quad t \in [0,\overline{T}),\ \overline{T} = 0.5\,.$$

For this evolution, we compare our results from (2.4a), (2.5) to the semi-implicit scheme (2.7a), (2.8), see Table 1. We use $\tau = 0.5\,h^2$, $T = \frac{1}{2}\,\overline{T}$ and compute the error $\|\vec{X} - \vec{x}\|_{L^\infty} := \max_{m=1\to M} \|\vec{X}(t_m) - \vec{x}(\cdot,t_m)\|_{L^\infty}$, where $\|\vec{X}(t_m) - \vec{x}(\cdot,t_m)\|_{L^\infty} := \max_{j=1\to J} \min_{\rho\in I} |\vec{X}^m(q_j) - \vec{x}(\rho,t_m)|$ between $\vec{X}$ and the true solution on the interval $[0,T]$. For both schemes we observe the expected quadratic rate of convergence, with the errors for the fully implicit scheme in general being smaller due to the slightly better observed convergence rate.

Our first computation for surface diffusion is for an initial curve in the shape of a tube with total dimensions 2×1. The discretization parameters are $J = 128$, $\tau = 10^{-4}$ and $T = 2$. The results for our approximation (2.4b), (2.5) are shown in Figure 2, together with a comparison for the semi-implicit scheme (2.7b), (2.8) from [11]. In particular, we show the evolution of Γ^m, as well as plots of the length $|\Gamma^m|$, and the element ratio

$$r^m := \frac{\max_{j=1\to J} |\vec{h}_j^m|}{\min_{j=1\to J} |\vec{h}_j^m|}\,. \tag{4.1}$$

As noted previously, the results from the two approximations are graphically indistinguishable, and so we only show the ratio plot r^m for the semi-implicit scheme. As expected, we see that the solution of (2.4b), (2.5) remains equidistributed at all times, while the approximation (2.7b), (2.8) from [11] only equidistributes the vertices asymptotically, once a steady state solution is reached. Moreover, we note that for this flow, as well as for all

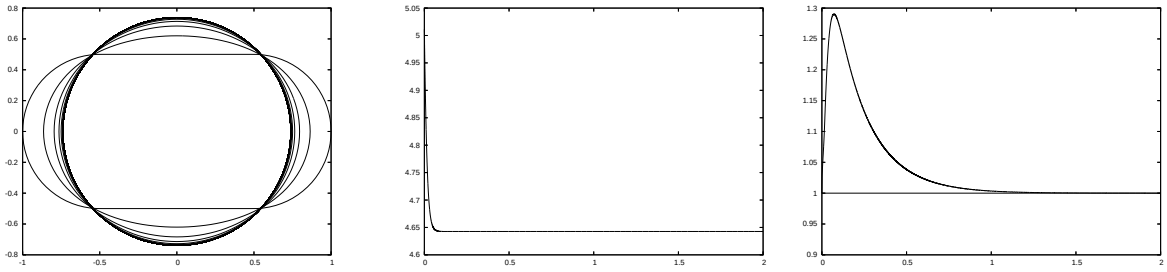

Figure 2: Evolution for (2.4b), (2.5). Plots of $\vec{X}(t)$, $t = 0, 0.02, \ldots, 2$, and plots of $|\Gamma^m|$ as well as the element ratio r^m, superimposed with r^m for (2.7), (2.8).

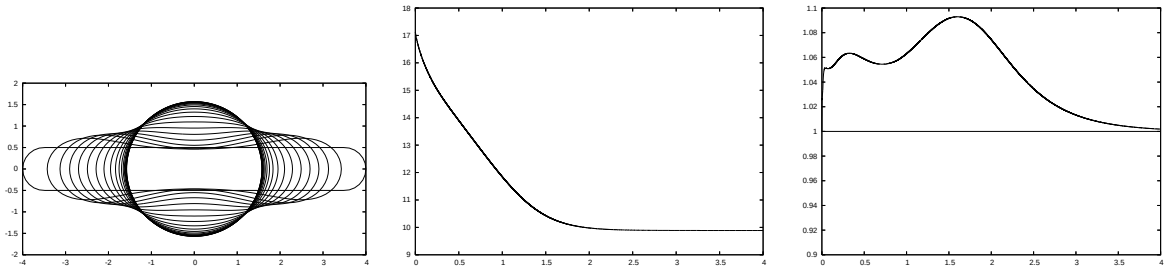

Figure 3: Evolution for (2.4b), (2.5). Plots of $\vec{X}(t)$, $t = 0, 0.2, \ldots, 4$, and plots of $|\Gamma^m|$ as well as the element ratio r^m for both (2.4b), (2.5) and (2.7b), (2.8).

the other experiments in this section, the numerical results from the two schemes (2.4b), (2.5) and (2.16b), (2.17) were identical (up to rounding errors and tolerances). This is not surprising, as for the flows considered in this paper, the curves Γ^{m+1}, $m = 0 \to M-1$, will never be locally flat. For this first numerical experiment, we also compared the performance of the two iterations (3.1b), (3.2) and (3.3b), (3.4). As noted previously, the results obtained from the two iterations are basically the same. However, while the former iteration took a maximum of 4210 iteration steps per time step, the latter never needed more than eight iteration steps.

As a further example, in Figure 3 we show the evolution of an initial tube of total dimensions 8×1. All the discretization parameters are as before. Once again, the nonlinear iterative solver (3.3b), (3.4) never needed more than eight iterations per time step. As a comparison, the same evolution for the semi-implicit scheme (2.7b), (2.8) from [11] is also shown in Figure 3.

4.1 Curve Networks

In Figure 4 we present a result for the scheme (2.24b), (2.25). As the iterative solver we use an algorithm similar to (3.3b), (3.4), so that we actually find a solution to (2.28,b), (2.29). As the initial curve network we choose the union of a unit circle and a straight line. As expected, the flow soon reaches a steady state, which is given by a standard double bubble. The discretization parameters are $\sum_{i=1}^{3} J_i = 255$, $\tau = 10^{-4}$ and $T = 0.5$. The nonlinear iterative solver never needed more than 12 steps. As a comparison, we also show the corresponding results for the semi-implicit scheme from [11] in Figure 4. In both cases we report on the ratio r^m, which here, similarly to (4.1), is defined by

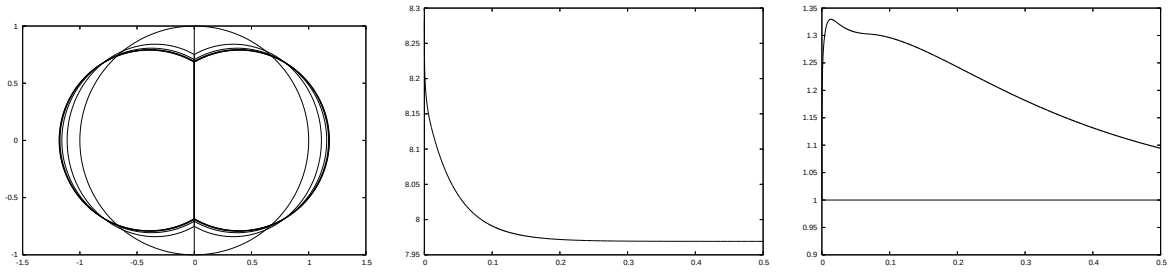

Figure 4: Evolution for (2.24b), (2.25). Plots of $\vec{X}(t)$, $t = 0, 0.1, \ldots, 0.5$, and plots of $|\Gamma^m|$ as well as the element ratio r^m for both (2.24b), (2.25) and for the scheme from [11].

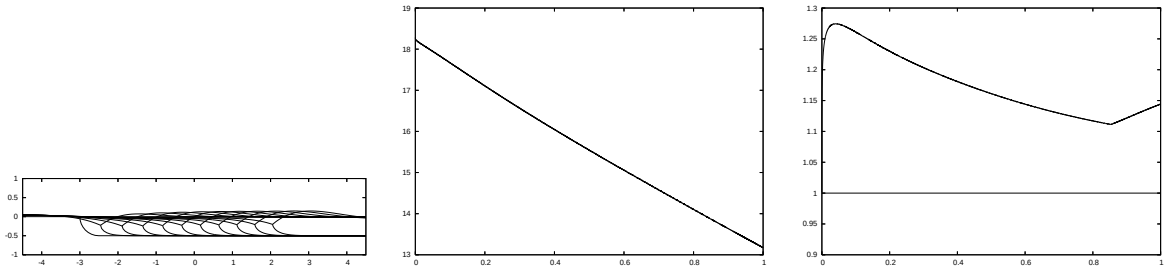

Figure 5: Evolution for the analogue of (2.24a,b), (2.25) for the flow (2.23). Plots of $\vec{X}(t)$, $t = 0, 0.1, \ldots, 1$, and plots of $|\Gamma^m|$ as well as the element ratio r^m for both the fully implicit scheme and for the semi-implicit scheme from [12].

$r^m := \max_{i=1\to 3} \frac{\max_{j=1\to J_i} |\vec{h}_j^{m,i}|}{\min_{j=1\to J_i} |\vec{h}_j^{m,i}|}$. It can be seen that even close to the numerical steady state, the semi-implicit scheme from [11] does not reach an equidistributed state on each Γ_i^m, $i = 1 \to 3$. This is caused by the straight lined curve, on which no equidistribution can be expected for that scheme.

In addition, we repeat the first experiment in [12, Fig. 28] for the gradient flow (2.23) of (2.21), see also [30, Fig. 2]. For the same discretization parameters as above, we show the evolutions for the natural analogue of the schemes (2.24a,b), (2.25) in Figure 5, together with a comparison for the semi-implicit counterpart from [12]. Like in all the other presented computations so far, the fully implicit scheme equidistributes the nodes exactly. We recall that when employing fully implicit time stepping and centred finite differences the same can be shown for the alternative numerical method for (2.23) in [25].

4.2 Anisotropic surface energies

Unless otherwise stated, we set $\beta \equiv 1$ throughout this section. For the anisotropy

$$\gamma(\vec{p}) = [\varepsilon^2\, p_1^2 + p_2^2]^{\frac{1}{2}}\,, \quad \varepsilon = \tfrac{1}{2}\,, \tag{4.2}$$

we repeated the experiment in Figure 3 for the same set of discretization parameters. As the chosen anisotropy γ satisfies (2.48), we can employ the iterative scheme (3.14b). In this experiment, and in all the other experiments for anisotropies of the form (2.34), we started with a polygonal approximation of $\Gamma(0)$ that almost satisfies (2.46b). To this end, we performed several "time steps" of the linear, semi-implicit scheme (3.13a,b),

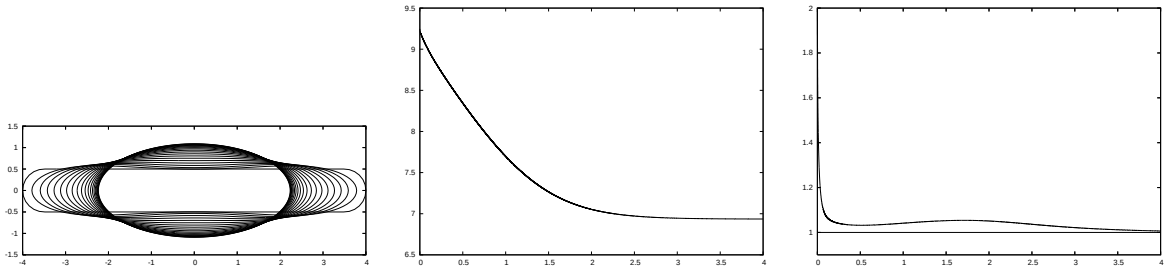

Figure 6: Evolution for (2.38b), (2.39). Plots of $\vec{X}(t)$, $t = 0, 0.2, \ldots, 4$, and plots of $|\Gamma^m|_\gamma$ as well as the anisotropic element ratio r_γ^m for both (2.38b), (2.39) and for the scheme from [31].

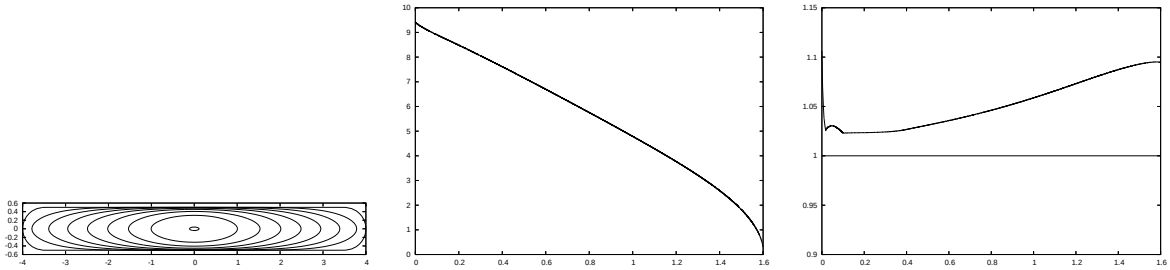

Figure 7: Evolution for (2.38a), (2.39). Plots of $\vec{X}(t)$, $t = 0, 0.2, \ldots, 1.6$, and plots of $|\Gamma^m|_\gamma$ as well as the anisotropic element ratio r_γ^m for both (2.38a), (2.39) and for the scheme from [31].

starting with an equistributed polygonal approximation of $\Gamma(0)$, until a numerical steady state is obtained. This steady state will satisfy (2.46b) up to a tolerance. The resulting curve is then projected back orthogonally to $\Gamma(0)$, so that the criterion will in general no longer hold. However, in practice this was sufficient to allow a fast iterative solve of the considered evolution equations, even for the first time step. For example, in the present experiment only 18 iterations were needed by the iterative solver (3.14b) to find $\Gamma^1 = \vec{X}^1(I)$. If we had started the experiment with an equidistributed approximation of $\Gamma(0)$, on the other hand, then the first time step would have needed more than 1500 iterative steps. Thereafter, the iteration (3.14b) never needed more than 13 iterations. In comparison, the iterative solver (3.12b) for the initial curve Γ^0 that almost satisfies (2.46c) needed more than 2031 steps for the first time step, and up to 1994 iterations for the subsequent steps. The iteration (3.10b), (3.11) did not converge for this experiment and for this set of parameters, and only converged on reducing the time step size τ sufficiently. The evolution of this experiment together with plots of the energy $|\Gamma^m|_\gamma$ and the anisotropic element ratio $r_\gamma^m := \frac{\max_{j=1\to J} \gamma([\vec{h}_j^m]^\perp)}{\min_{j=1\to J} \gamma([\vec{h}_j^m]^\perp)}$ are shown in Figure 6. A comparison for the semi-implicit scheme from [31] is shown in the same figure.

A run for the corresponding curvature flow experiment, i.e. starting with the same initial curve and using the same discretization parameters, is shown in Figure 7. For the iterative solver (3.14a) the computation of $\Gamma^1 = \vec{X}^1(I)$ needed 20 iteration steps, with the following time levels being found within less than 14 iterations. As a comparison, we show the evolution for the semi-implicit scheme from [31] in the same figure.

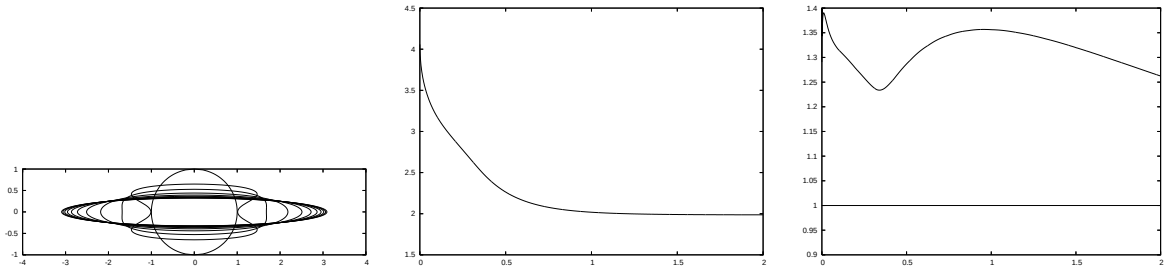

Figure 8: Evolution for (2.38b), (2.39). Plots of $\vec{X}(t)$, $t = 0, 0.2, \ldots, 2$, and plots of $|\Gamma^m|_\gamma$ as well as the anisotropic element ratio r_γ^m for both (2.38b), (2.39) and for the scheme from [31].

In addition, we repeated the experiment in [31, Fig. 8], i.e. an experiment for the flow (2.37b) for a unit circle and for the anisotropy (4.2) with $\varepsilon = 0.1$. The discretization parameters are $J = 128$, $\tau = 10^{-3}$ and $T = 2$. The evolution of this experiment together with plots of the energy $|\Gamma^m|_\gamma$ and the anisotropic element ratio r_γ^m are shown in Figure 8. A comparison for the semi-implicit scheme from [31] is also shown in Figure 8. Once again we observe that the results from the two schemes are very similar, the only striking difference being that the fully implicit scheme (2.38b), (2.39) equidistributes the vertices with respect to γ at every time step, while the semi-implicit scheme will do so only in the asymptotic limit, when it reaches a numerical steady state.

For the next experiments we consider as anisotropy the regularized l^1-norm

$$\gamma(\vec{p}) = \sum_{i=1}^{2} \left[\varepsilon^2 \left|\vec{p}\right|^2 + p_i^2(1-\varepsilon^2)\right]^{\frac{1}{2}}, \quad \varepsilon = \tfrac{1}{2}, \tag{4.3}$$

which is clearly of the form (2.34), with $L = 2$, but not of the form (2.48). Hence we employ the iterative solvers (3.12a,b) in order to find a solution of the nonlinear algebraic systems at each time level. A repeat of the experiment in Figure 7, now for the anisotropy (4.3), is shown in Figure 9. For the iterative solver (3.12a), the computation of $\Gamma^1 = \vec{X}^1(I)$ needed 2913 iteration steps, with the following time levels being found within less than 3386 iterations. As a comparison, we show the evolution for the semi-implicit scheme from [31] also in Figure 9. Here it is interesting to note that the condition (2.46b) for this example does indeed not yield equidistribution with respect to γ. In particular, the weighted element ratio r_γ^m in this experiment is never smaller than 1.2. Indeed, it does not even stay constant throughout the evolution.

Moreover, we performed an experiment for the anisotropy (4.3) with $\varepsilon = \frac{1}{4}$ for the evolution under surface diffusion of a unit circle to the Wulff shape. The discretization parameters are $J = 128$, $\tau = 10^{-3}$ and $T = 0.5$. The iterative solver (3.12b) needed 10688 iterations in the first time step, and up to 8969 iterations in the steps thereafter. Of course, once the evolution has settled on a numerical steady state, then the nonlinear solver finds the solution in only one step. The results are shown in Figure 10, and as a comparison, we also show the evolution for the semi-implicit scheme from [31]. In this experiment, the fully implicit scheme (2.38b), (2.39) soon finds a numerical steady state, with the element ratio $r_\gamma^m \approx 1.99$. The semi-implicit scheme from [31], on the other hand,

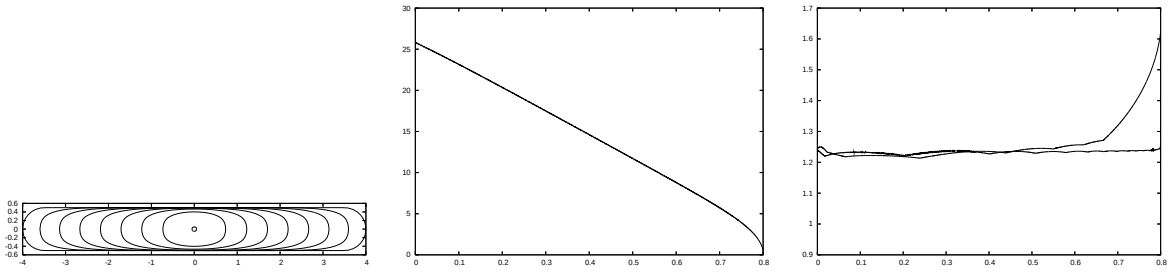

Figure 9: Evolution for (2.38a), (2.39). Plots of $\vec{X}(t)$, $t = 0, 0.1, \ldots, 0.8$, and plots of $|\Gamma^m|_\gamma$ as well as the anisotropic element ratio r_γ^m for both (2.38a), (2.39) and for the scheme from [31].

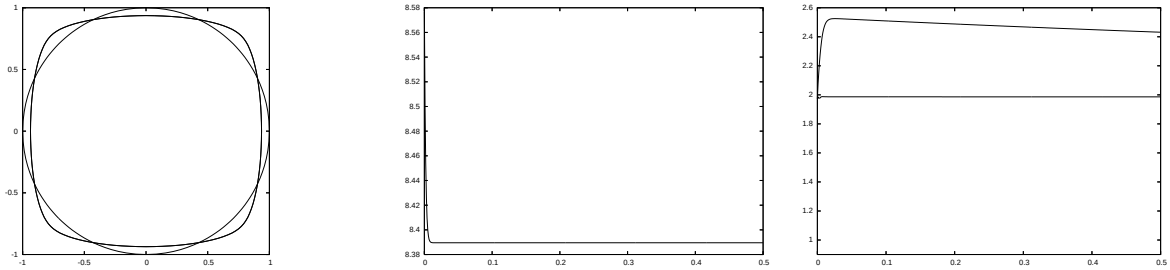

Figure 10: Evolution for (2.38b), (2.39). Plots of $\vec{X}(t)$, $t = 0, 0.2, 0.4, 0.5$, and plots of $|\Gamma^m|_\gamma$ as well as the anisotropic element ratio r_γ^m for both (2.38b), (2.5) and for the scheme from [31].

still moves the vertices tangentially, as at time $T = 0.5$ it still does not satisfy the criterion (2.46b).

We remark that we were so far unable to compute an example for the schemes (2.38a,b), (2.39) for a general smooth and convex anisotropy that is not of the class (2.34). The main obstacles are to find a robust solution method for the nonlinear systems of equations (2.38a,b), (2.39). The candidates (3.10a,b), (3.11) did not work well in practice, and for anisotropies of the form (2.34) these iterations in general performed worse than (3.12a,b). Moreover, even for a good nonlinear iterative solver it is to be expected that the initial guess needs to be sufficiently close to the sought solution. In particular, the initial guess should (almost) satisfy the criterion (2.46a). However, in the absence of a stable semi-implicit scheme such as (3.13a,b) for the class (2.34), it is again nontrivial how to obtain such an initial guess.

Finally, we consider the schemes (2.56a,b) and (2.58a,b) for some general anisotropies. Here we choose $\gamma(\vec{\nu}) \equiv \gamma(\cos\theta, \sin\theta) = \widehat{\gamma}(\theta)$ with either

$$\widehat{\gamma}(\theta) = 1 + \delta\, \cos(k\,\theta)\,, \qquad \delta \in \mathbb{R}_{\geq 0},\, k \in \mathbb{N}\,, \tag{4.4a}$$

or

$$\widehat{\gamma}(\theta) = 1 + \delta\, \left[\cos^2(\tfrac{k}{2}\,\theta) + \varepsilon^2\right]^{\frac{1}{2}}\,, \qquad \delta \in \mathbb{R}_{\geq 0},\, k \in \mathbb{N},\, \varepsilon \in \mathbb{R}_{>0}\,. \tag{4.4b}$$

On recalling that $a(\vec{\nu}) = \widehat{\gamma}''(\theta) + \widehat{\gamma}(\theta)$, we note that for (4.4a) the assumptions (2.57) are satisfied if and only if $\delta \leq (k^2 - 1)^{-1}$, i.e. γ becomes nonconvex for larger choices of δ. For the anisotropy (4.4b) no such simple strict bound appears to be available, and so in

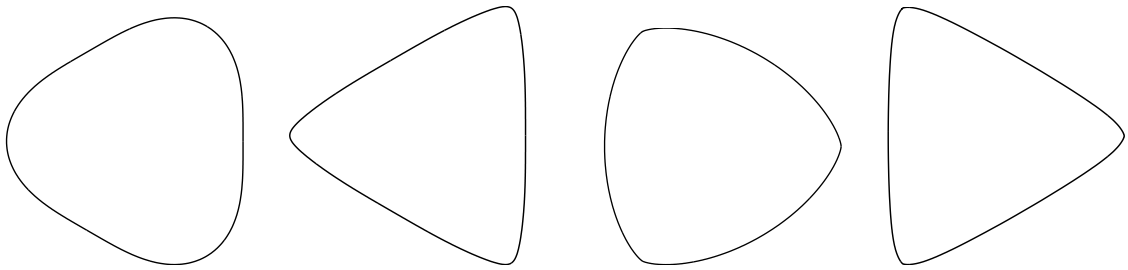

Figure 11: Frank diagrams (left) and Wulff shapes (right) for (4.4a,b). On the left (4.4a) with $k = 3$, $\delta = 0.125$ and on the right (4.4b) with $k = 3$, $\delta = 0.8$ and $\varepsilon = 0.1$.

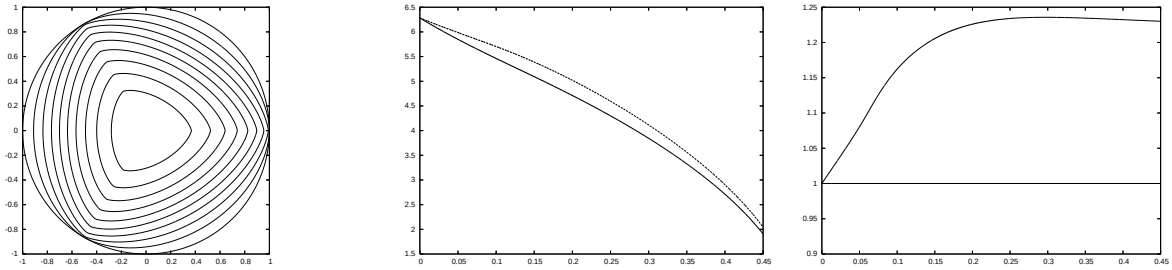

Figure 12: Evolution for (2.56a,b) and (4.4a) with $k = 3$ and $\delta = 0.125$. Plots of $\vec{X}(t)$, $t = 0, 0.05, \ldots, 0.45$ and plots of $|\Gamma^m|_\gamma$ (solid) superimposed with $|\Gamma^m|$ (dashed) as well as a plot of the isotropic element ratio r^m for (2.56a,b) and (2.60).

practice we monitor whether the quantity

$$\widehat{\gamma}''(\theta) + \widehat{\gamma}(\theta) = 1 + \delta \left[\cos^2(\tfrac{k}{2}\,\theta) + \varepsilon^2\right]^{\frac{1}{2}} \Big[1 - \tfrac{k^2}{4} \left[\cos^2(\tfrac{k}{2}\,\theta) + \varepsilon^2\right]^{-1} \cos(k\,\theta) \\ - \tfrac{k^2}{16} \left[\cos^2(\tfrac{k}{2}\,\theta) + \varepsilon^2\right]^{-2} \sin^2(k\,\theta)\Big]$$

remains nonnegative. For small ε the choice (4.4b) yields a smoothed regularization of the crystalline anisotropy $\widehat{\gamma}(\theta) = 1 + \delta\,|\cos(\frac{k}{2}\,\theta)|$, whose Wulff shape for sufficiently large δ approximates a regular k-polygon. For the reader's convenience, we show some example Frank diagrams $\mathcal{F} := \{\vec{p} \in \mathbb{R}^2 : \gamma(\vec{p}) \leq 1\}$ and Wulff shapes $\mathcal{W} := \{\vec{p} \in \mathbb{R}^2 : \vec{p}\,.\,\vec{q} \leq \gamma(\vec{q}) \quad \forall\, \vec{q} \in \mathbb{R}^2\}$ for the two anisotropies (4.4a,b) with $k = 3$ in Figure 11.

In Figure 12 we show the shrinking of a unit circle under the flow (2.54a) for the anisotropy (4.4a) as depicted in Figure 11. The discretization parameters for this and the following experiments are $J = 1024$ and $\tau = 10^{-4}$. For this experiment, the iterative solver (3.15), (3.4) never needed more than six iterations per time step. As usual, we also report on the corresponding results for the semi-implicit scheme (2.60) in Figures 12. The same experiments for the anisotropy (4.4b) with $k = 5$ and $\delta = 0.19$, for which (2.57) in practice was satisfied, can be seen in Figure 13.

Finally we perform an experiment for the anisotropic surface diffusion flow (2.54b) for the anisotropy (4.4b) as depicted in Figure 11. The initial curve is given as in the experiment in Figure 6. The results for the scheme (2.58a,b), as well as its semi-implicit counterpart, are shown in Figure 14. We observe that, as expected, the curve flows towards the Wulff shape and that in this experiment the weighted length $|\Gamma^m|_\gamma$ decreased monotonically, even though we do not have a stability proof for (2.58a,b).

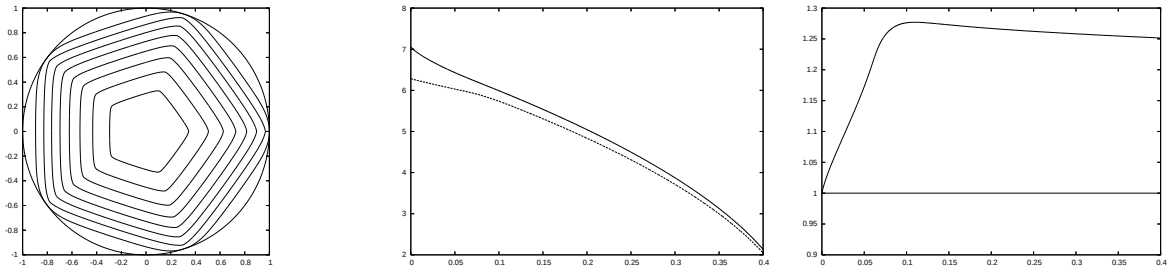

Figure 13: Evolution for (2.56a,b) and (4.4b) with $k = 5$ and $\delta = 0.19$. Plots of $\vec{X}(t)$, $t = 0, 0.05, \ldots, 0.4$ and plots of $|\Gamma^m|_\gamma$ (solid) superimposed with $|\Gamma^m|$ (dashed) as well as a plot of the isotropic element ratio r^m for (2.56a,b) and (2.60).

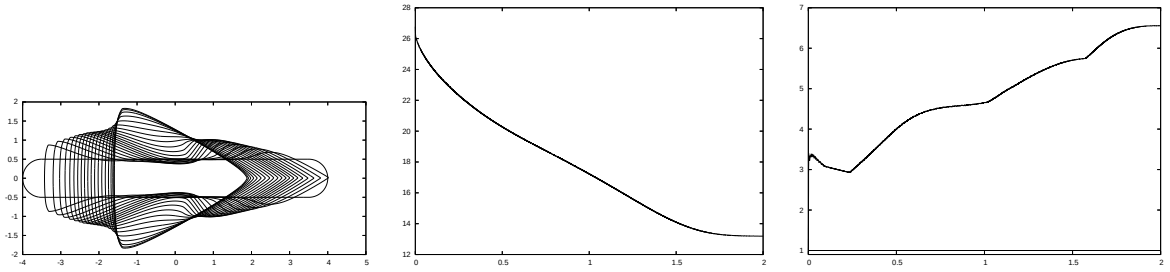

Figure 14: Evolution for (2.58a,b) and (4.4b) with $k = 3$ and $\delta = 0.8$. Plots of $\vec{X}(t)$, $t = 0, 0.1, \ldots, 2$ and plots of $|\Gamma^m|_\gamma$ and the isotropic element ratio r^m for (2.58a,b) and its semi-implicit counterpart.

5 Conclusions

We have presented fully discrete, fully implicit finite element approximations for the motion by curvature and motion by surface diffusion of curves in $\mathbb{R}^2$. The presented schemes are unconditionally stable and intrinsically move the vertices tangentially along the curve, so that the vertices are equidistributed at every time step. Generalizations to many more general evolution equations are possible, and we have sketched the details for the case of curve networks and the case of anisotropic surface energies. A presented iterative solver for the highly nonlinear algebraic equations in practice always converged for isotropic and simple anisotropic surface energies. However, developing a more robust solution method that works well for a larger class of anisotropies, as well as extending the ideas presented here to the evolution of hypersurfaces in $\mathbb{R}^3$ remains a challenging task for the future.

The presented numerical experiments revealed that in practice the results from the novel fully implicit approximations introduced in this paper and from the corresponding semi-implicit approximations are in general graphically indistinguishable. Given that for the semi-implicit schemes only a linear system of equations needs to be solved at each time level, given that they satisfy the same stability bounds as the fully-implicit schemes, and given that there is no noticeable deterioration of the mesh quality, from a practical point of view it will often make sense to use the corresponding semi-implicit approximations, rather than the fully implicit schemes introduced in this paper. However, studying the newly introduced fully implicit finite element approximations gives valuable

theoretical insights, and in many aspects they improve on previous numerical methods in the literature that attempt to achieve an equidistribution of vertices.

References

[1] K. Deckelnick, G. Dziuk, and C. M. Elliott, *Computation of geometric partial differential equations and mean curvature flow*, Acta Numer., 14 (2005), pp. 139–232.

[2] G. Dziuk, *An algorithm for evolutionary surfaces*, Numer. Math., 58 (1991), pp. 603–611.

[3] ——, *Convergence of a semi-discrete scheme for the curve shortening flow*, Math. Models Methods Appl. Sci., 4 (1994), pp. 589–606.

[4] K. Deckelnick and G. Dziuk, *On the approximation of the curve shortening flow*, in Calculus of Variations, Applications and Computations (Pont-à-Mousson, 1994), vol. 326 of Pitman Res. Notes Math. Ser., Longman Sci. Tech., Harlow, 1995, pp. 100–108.

[5] K. Deckelnick and C. M. Elliott, *Finite element error bounds for a curve shrinking with prescribed normal contact to a fixed boundary*, IMA J. Numer. Anal., 18 (1998), pp. 635–654.

[6] G. Dziuk, *Discrete anisotropic curve shortening flow*, SIAM J. Numer. Anal., 36 (1999), pp. 1808–1830.

[7] G. Dziuk, E. Kuwert, and R. Schätzle, *Evolution of elastic curves in $\mathbb{R}^n$: existence and computation*, SIAM J. Math. Anal., 33 (2002), pp. 1228–1245.

[8] E. Bänsch, P. Morin, and R. H. Nochetto, *A finite element method for surface diffusion: the parametric case*, J. Comput. Phys., 203 (2005), pp. 321–343.

[9] P. Pozzi, *Anisotropic curve shortening flow in higher codimension*, Math. Methods Appl. Sci., 30 (2007), pp. 1243–1281.

[10] K. Deckelnick and G. Dziuk, *Error analysis for the elastic flow of parametrized curves*, Math. Comp., 78 (2009), pp. 645–671.

[11] J. W. Barrett, H. Garcke, and R. Nürnberg, *A parametric finite element method for fourth order geometric evolution equations*, J. Comput. Phys., 222 (2007), pp. 441–467.

[12] ——, *On the variational approximation of combined second and fourth order geometric evolution equations*, SIAM J. Sci. Comput., 29 (2007), pp. 1006–1041.

[13] ——, *Numerical approximation of gradient flows for closed curves in $\mathbb{R}^d$*, IMA J. Numer. Anal., (2009). doi:10.1093/imanum/drp005, (to appear).

[14] R. E. Rusu, *Numerische Analysis für den Krümmungsfluß und den Willmorefluß*, PhD thesis, University Freiburg, Freiburg, 2006.

[15] J. A. Sethian, *Curvature and the evolution of fronts*, Comm. Math. Phys., 101 (1985), pp. 487–499.

[16] D. A. Kessler, J. Koplik, and H. Levine, *Pattern selection in fingered growth phenomena*, Adv. Phys., 37 (1988), pp. 255–339.

[17] ——, *Numerical simulation of two-dimensional snowflake growth*, Phys. Rev. A, 30 (1984), pp. 2820–2823.

[18] J. Strain, *A boundary integral approach to unstable solidification*, J. Comput. Phys., 85 (1989), pp. 342–389.

[19] T. Y. Hou, J. S. Lowengrub, and M. J. Shelley, *Removing the stiffness from interfacial flows with surface tension*, J. Comput. Phys., 114 (1994), pp. 312–338.

[20] T. Y. Hou, I. Klapper, and H. Si, *Removing the stiffness of curvature in computing* 3*-D filaments*, J. Comput. Phys., 143 (1998), pp. 628–664.

[21] M. Kimura, *Accurate numerical scheme for the flow by curvature*, Appl. Math. Lett., 7 (1994), pp. 69–73.

[22] ——, *Numerical analysis of moving boundary problems using the boundary tracking method*, Japan J. Indust. Appl. Math., 14 (1997), pp. 373–398.

[23] K. Mikula and D. Ševčovič, *Evolution of plane curves driven by a nonlinear function of curvature and anisotropy*, SIAM J. Appl. Math., 61 (2001), pp. 1473–1501.

[24] ——, *Tangentially stabilized Lagrangian algorithm for elastic curve evolution driven by intrinsic Laplacian of curvature*, in ALGORITMY 2005, A. Handlovicova, Z. Kriva, K. Mikula, and D. Ševčovič, eds., Bratislava, 2005, Slovak University of Technology, pp. 32–41.

[25] Z. Pan and B. Wetton, *A numerical method for coupled surface and grain boundary motion*, European J. Appl. Math., 19 (2008), pp. 311–327.

[26] Z. Pan, *Simulation and Analysis of Coupled Surface and Grain Boundary Motion*, PhD thesis, University of British Columbia, Vancouver, 2008.

[27] J. W. Barrett, H. Garcke, and R. Nürnberg, *On the parametric finite element approximation of evolving hypersurfaces in* $\mathbb{R}^3$, J. Comput. Phys., 227 (2008), pp. 4281–4307.

[28] ——, *Parametric approximation of Willmore flow and related geometric evolution equations*, SIAM J. Sci. Comput., 31 (2008), pp. 225–253.

[29] ——, *Parametric approximation of surface clusters driven by isotropic and anisotropic surface energies*, 2009. Preprint No. 04/2009, University Regensburg.

[30] ——, *Finite element approximation of coupled surface and grain boundary motion with applications to thermal grooving and sintering*, 2009. Preprint No. 11/2009, University Regensburg.

[31] ——, *Numerical approximation of anisotropic geometric evolution equations in the plane*, IMA J. Numer. Anal., 28 (2008), pp. 292–330.

[32] ——, *On stable parametric finite element methods for the Stefan problem and the Mullins–Sekerka problem with applications to dendritic growth*, 2009. Preprint No. 21/2009, University Regensburg.

[33] J. Pan, *Modelling sintering at different length scales*, Int. Mater. Rev., 48 (2003), pp. 69–85.

[34] W. W. Mullins, *The effect of thermal grooving on grain boundary motion*, Acta Metall., 6 (1958), pp. 414–427.

[35] J. W. Cahn, *Stability, microstructural evolution, grain growth, and coarsening in a two-dimensional two-phase microstructure*, Acta Metall., 39 (1991), pp. 2189–2199.

[36] J. W. Barrett, H. Garcke, and R. Nürnberg, *A phase field model for the electromigration of intergranular voids*, Interfaces Free Bound., 9 (2007), pp. 171–210.

[37] ——, *A variational formulation of anisotropic geometric evolution equations in higher dimensions*, Numer. Math., 109 (2008), pp. 1–44.

[38] J. W. Cahn and D. W. Hoffmann, *A vector thermodynamics for anisotropic surfaces – II. curved and faceted surfaces*, Acta Metall., 22 (1974), pp. 1205–1214.

[39] C. M. Elliott, *Approximation of curvature dependent interface motion*, in The state of the art in numerical analysis (York, 1996), vol. 63 of Inst. Math. Appl. Conf. Ser. New Ser., Oxford Univ. Press, New York, 1997, pp. 407–440.

[40] X. Wu, *Note on the improvement of Newton's method for system of nonlinear equations*, Appl. Math. Comput., 189 (2007), pp. 1476–1479.